Synthesis of ZnO and C-doped ZnO Nanowires for Future Spintronics Applications

by

Aman Ullah

A dissertation submitted in partial fulfillment of the requirements

for the degree of Master of Philosophy in Physics
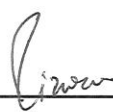
Supervised by

Dr. Qurat ul Ain

School of Natural Sciences (SNS)

National University of Sciences and Technology

Islamabad, Pakistan

National University of Sciences & Technology

M.Phil THESIS WORK

We hereby recommend that the dissertation prepared under our supervision by: Aman Ullah, Regn No. NUST201361980MSNS7811F Titled: Synthesis of ZnO and C-doped ZnO Nanowires for Future Spintronics Applications be accepted in partial fulfillment of the requirements for the award of **M.Phil** degree.

Examination Committee Members

1. Name: Dr. Zahida Malik   Signature: _____

2. Name: Dr. Rizwan Hussain   Signature: _____

3. Name: _____   Signature: _____

4. Name: Dr. M. Kashif Nadeem   Signature: _____

Supervisor's Name: Dr. Qurat ul Ain   Signature: _____

_____
Head of Department

02-02-16
Date

COUNTERSINGED

Date: 02/02/16

_____
Dean/Principal

Dedicated to my parents,

who valued my education above all else

Acknowledgements

Abstract

Spin injection in semiconductor material produces highly spin polarized current with long spin diffusion length which is useful for spintronics applications. ZnO is a wide band gap semiconductor material, doping of carbon introduces n-type vacancy in it. This n-type vacancy produces a highly spin polarized current with long spin diffusion length. Spin diffusion length is to be calculated through dielectric measurement. Synthesis of such system requires control on the nucleation of the system. Synthesis of ZnO and C-ZnO nanowires has been carried out through hydrothermal process in surfactant assisted control growth, Polyethylene Glycol (PEG) is used as surfactant. By varying the percentage of PEG from 1% to 15%, surface energy varies from 11.385j/m^2 to 8.785j/m^2, at 5% to 10% of PEG surface energy modulates between 10.385j/m^2 to 9.785j/m^2 which allows the carbon to makes a bond with ZnO. FTIR spectroscopy is used to analyzed the bonds present in ZnO. Optical properties are studied thorough UV-Vis spectroscopy, which gave band gap energy tuned from E_g= 3.4062 eV to E_g= 3.3783 eV for ZnO, when carbon is introduced as a dopant material. Further structural morphology is studied through SEM analysis for ZnO and C-ZnO. SEM analysis confirms that one dimensional nanowires are formed for both ZnO and C-ZnO at 5% and 10% of PEG. Elemental composition is analyzed through EDX spectroscopy. Crystallinity of ZnO and C-ZnO is analyzed through XRD spectroscopy. Dielectric properties are studied through LCR meter, dielectric constant for C-ZnO is greater than ZnO, which produces long spin diffusion length. Materials having long spin diffusion length is to be used as quantum channel in spintronics devices such as physical implementation of 2 qubit gate.
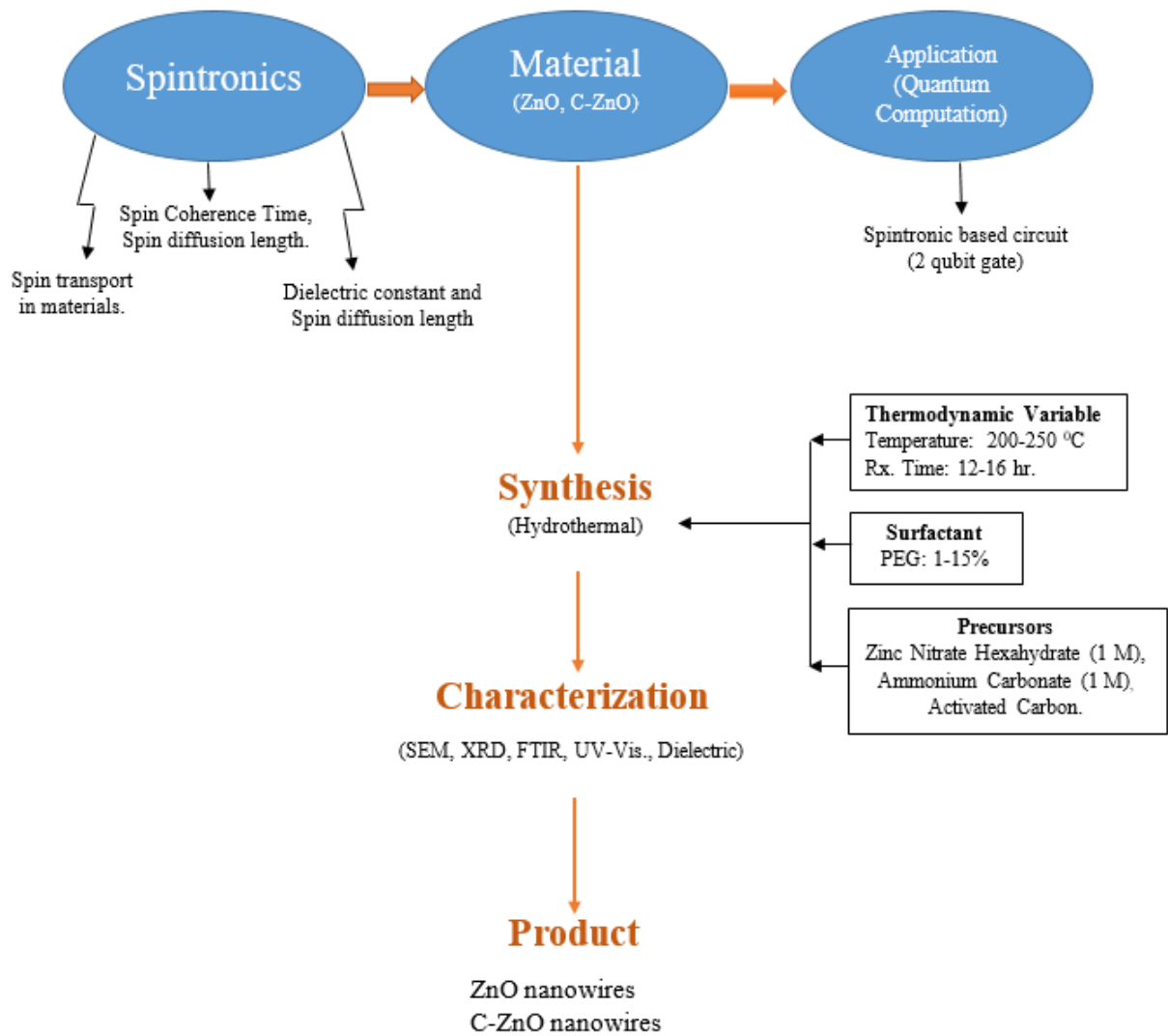
Graphical Abstract

Figure 1: Graphical Abstract for Synthesis of ZnO and C-doped ZnO nanowires and its Applications in Spintronics

Contents

4

List of Figures

6

List of Tables

Notations and conventions

$\uparrow$	Spin-up electron
$\downarrow$	Spin down electron
$n_\uparrow$	Spin density for spin-up electron
$n_\downarrow$	Spin density for spin down electron
$\tau_{\downarrow\uparrow}$	Spin relaxation time
t_1	Longitudinal spin relaxation time
t_2	Transverse spin relaxation time
T_l	Decoherence time
L_D	Spin diffusion length
g	Lande's splitting factor
Ω	Precessional frequency
$\sigma(\theta, E)$	Scattering cross section
τ	Effective time for field reversal
α_i	Thermal expansion coefficient
$\sigma_{\alpha\beta}$	Interfacial energy
DMS	Dilute magnetic semiconductor
CNOT	Control-Not
LDA	Local density approximation
RTF	Room temperature ferromagnetism
STT	Spin transfer torque
C-ZnO	Carbon doped ZnO
PEG	Poly ethylene Glycol

1-D   Nanowires

2-D   Thin films

MRAM   Magnetoresistive random-access memory

TMR   Tunneling magnetoresistance

GMR   Giant magnetoresistance

Introduction

Recent computers based on silicon technology dealt with charge manipulation, and bit information are stored on high and low flow of charges or presence and absence of charges. Advancement in recent computers needs the reduction of size, plus getting more computation power. As for the concern of reduction of size there is problem with thermal instability in other words there is leakage of information when confinement of degree of freedom for charges in reduced dimensions are done. So computation power can be limited up to some extent. Although there are solutions which can compensate these problems up to some limits, solution like for the successful fabrication of single electron with the help of nanotechnology and using quantum mechanics formalism such as designing desired function Hamiltonian which can breached the limit. But these solutions are difficult or sometimes even impossible to implement experimentally. Rather reducing the size of existing silicon based devices there is another way around which deals with introducing spin to the charges in other words introducing another degree of freedom.

Spin injection in semiconductor material produces highly spin polarized current, which provides one of the way to implement quantum computation physically. So there is a need to control the spin transport in materials along with charge. As spin has two distinct eigenvalues (up, down) and measurement results in any one of these values, in other words at any instant your state is to be in a superposition of spin up and spin down eigenvalues which we call a quantum bit. For any quantum gate operation all spins must have any one of the eigenvalue after measurement which generates a

polarized current. In other words polarization is achieved when all the surroundings spins resulted in same eigenvalues. Due to thermal fluctuation coherence between different spins decayed which causes a unpolarized current. So coherence time should be enough such that in which quantum gate operation can be performed. Ferromagnetic materials have spins aligned in specific direction, which is big source of coherence. [1]

So there are need to search for such materials through which spin injection and spin transport can be made possible, one way is to dope a transition metals in semiconductor materials which categorized in dilute magnetic semiconductor (DMS) and synthesized at nano-scale. Because at nano-scale as there few state are available so there is greater probability that all states remains coherent and resulted in one of the eigenvalue after measurement, and polarized current can be achieved. DMSs have ferromagnetism at room temperature, so practical quantum device can be fabricated. As doping of transition metals after specific percentage causes clustering and formation of secondary phases, which causes decoherence. There is another way to introduce magnetism in semiconductor by introducing n-type vacancy which can be achieved by doping of non-metals with low percentage. [2]

Spintronics or spin electronics is the study of spin manipulation along with charge manipulation through solid state system. It has some peculiarities which make it favorable:

1. Analogous to bit in classical computation, qubit is introduced which is superposition of up and down spin.

$$\psi = \alpha| \uparrow> +\beta| \downarrow> \tag{1.1}$$

$|\alpha|^2$ and $|\beta|^2$ gives probability amplitude for $\uparrow$ and $\downarrow$ spin respectively. α and β are the complex number and also defines the interference through different state in system, so resultant wave function consist of many different possible outcomes until the measurement is done. In other words resultant wave function is superposition of many computation carried out simultaneously. [3] Problems like prime factoring of large number, inversion of function, tractable etc. can be resolved.

2. Spin state can be controlled by magnetic as well as electric field, interaction with magnetic field used in giant magnetoresistance [4] and with electric field seen in Rashba effect which is used to flip the spin. [5]

3. Spin coherence time is enough to perform gate operations, however it decohere due to thermal fluctuation.

4. Any formulism can be formulated by making analogy between two state of spin with two band model for charges.

Materials incorporated both charge and spin properties known as dilute magnetic semiconductor (DMS) and provide appropriate conditions for spintronics applications. Such as logic devices, non-volatile magnetic memory storage, spin-emitting diode etc. These materials have ferromagnetism intrinsic in nature. Ferromagnetic materials have spin alignment in specific direction, which can be used for spintronics application. Nano-structured materials have properties between bulk and single atom, today's challenges of nanotechnology in the field of magnetism is to find appropriate conditions for materials at which it has both 'nano' and 'ferro' at the same time.

For device application ferromagnetism would exist at room temperature(RT). One way to synthesized nano structures of intrinsically available ferromagnetic materials such as Nikal (Ni), Iron (Fe), cobalt (Co) and alloys of these materials, or synthesizing the nano structures of hybrid materials such as ZnO, GaN etc and doping with transition metal. Because transition metal doped ZnO and GaN nano-structures have RT ferromagnetism. ZnO and GaN are semiconductor in nature and transition metal are magnetic in nature so both charge along spin manipulation can be achieved. Problem with transition metal doping that it forms clustering when little fluctuation in ambient condition, in other words secondary phases are formed which diminishes the magnetic properties.

As magnetism is related to spin angular momentum of electrons, spin is balanced out in ensembles or spin global quantization axis didn't found. There is another way around to generate magnetism and avoid secondary phases, that is to dope with such materials which make vacancies in materials. If we dope carbon in ZnO, then carbon tries to replace Zn and O but due large differences in atomic masses in carbon and Zn in other word's carbon has not enough momentum to replace Zn atom

from lattice site. Doping principle says that if doping is possible then dopant tries to replaces nearest atomic mass atoms in the crystal lattice. So carbon tries to replace Oxygen atoms in ZnO structure and creates isolated vacancies which have definite spin angular moment along with orbital angular momentum. And responsible for magnetism in ZnO. But the weight percentage of carbon should be low because of avoiding damaging of ZnO crystal structure.

Tunability of diameter in 1-D structure (nanowires) causes change in band gap, due to variation in band gap exchange interaction changes which is responsible for coherence in spin states. For ZnO as the diameter is decreased band gap increased hence exchange interaction increases, and spin states remains coherent for enough long time in which gate operations can be performed. Along with spin coherence time spin diffusion length should be considered for spin manipulation. [6]

Carbon doped ZnO nanowires can grown by using Vapor-Liquid-Solid method (VLS) which needs manually controlling of environmental conditions. But the control in diameter isn't efficient in this method. ZnO with tunability in diameter up to large extent can be synthesized using hydrothermal technique, but doping of carbon distort the ZnO nanowires. Carbon doping can be made possible through hydrothermal synthesis in the presence of appropriate percentage of surfactant. Surfactant function is to control the nucleation process, at specific percentage of it carbon atoms are allowed to replace oxygen atoms in ZnO. Different characterization like XRD, SEM, EDX has to be performed for the evidence of single phased ZnO and Carbon doped ZnO. Properties like optical and dielectric a has to be characterized using characterization tools UV-Vis, four-probe LCR meter respectively.

1.1   Spintronics and Quantum Computation

To find similarity between Quantum computation (QC) and Spintronics one would have to understand different prospects of both. One of the solid aspect is that, Quantum computating is all about information processing in a discrete manner and where as spintronics concern with spin transportation and there isn't any doubt that spin entity is quantized. So both have the quantization resemblance. So physical realization of QC based on spintronics needs some prerequisites to

fulfill;

1. Physical implementation of qubit.

2. Initialization qubit by fiducial state such as $|000\rangle$.

3. Coherence time such that gate operation can be computed before it decay.

4. Universal Quantum gate such as Hadamard (H) and Control-NOT (CNOT) gates can be implemented.

5. Qubit measurement capability.

6. Converting flying qubit to stationary.

7. High fidelity should be held in information transmission.

The first five relate to physical implementation of quantum computation while last two for manipulation for distinct computation. The realization of first can be thought of spin of carriers. In solid state physics spin coherence tie is long as compared to any other degree of freedom. In 6, 7 processing of information at long distance. For long distance photons are considered rather then electrons and keeping it faithfully. There are three three proposed model for Spin qubit:

1. Loss and DiVincenzo proposed that qubit can be thought of spin of electron or few electrons. [7] Kouwenhoven established an experiment based on quantum dots by controlling and characterizing the spin of electrons in other words controlling the qubit [8].

2. Kane proposed the qubit can be thought of isolated donor impurity such as 'P' and 'N' in semiconductor impurity [9].

   (Basic idea of both proposals is that considering the spin of weakly localized electrons and interaction of applied field changes the spin+orbital momentum and corresponding control on spin.)

3. Yablonovich made hybrid of both, in which donor impurity introduced by doping a magnetic material in semiconductor, which is Diluted Magnetic Semiconductor (DMS) [10].

4. Another approach is by considering the exciton as qubit. Steel and his co-worker showed experimentally that coherence time for exciton are not longer then spin coherence time but optical control are faster then electronic control [11].

Ideas which reveals the physical realization of qubit based on nuclear spin are no longer effective in spintronics 'Kane' himself regret the nuclear spin based qubit.

Spintronics provides podium to the physical implementation of Quantum Computation, Quantum gates such two qubit gate can be implemented physically. With the help of these gates complex circuits can be made and finally we can reach to final destination that is Quantum Computer. Well the purpose of Quantum Computer isn't only to fast computation but also to understand and enumerate the quantum nature of universe.

Chapter 2

Introduction to Spintronics and Literature review

According to Moor's law number of transistor on a silicon chip will approximately doubled in every eighteen months. In 2008 the width of electrode was about 48nm on microprocessor. As electronic devices become smaller and smaller quantum effects are no longer been ignored.

It is need to made advancement in current electronic device in a such a way that it can remove every hurdles. One way is by introduction of new degree of freedom, that is spin. This new degree of freedom along with charges explore new science known as Spintronics or Spinelectronics or Fluxtronics in which transportation of spin and associated magnetic moment in addition with fundamental transport of charges is been studied. This new degree of freedom possess enhancement in data storage, speed, low power consumption etc.

Such materials which exploit spin along with charge have triumphant injection, transport, manipulation, and detection of spin-polarized currents. And mobile carriers have long spin de-phasing time and large spin coherence length. Due to wide band gap of II-VI Semiconductor exhibit long coherence length and long spin life time can be achieved by doping with such materials which have intrinsic spin orbit coupling and hyperfine couplings. [12]

2.1 Transportation of Spin Density Packet:

Analogy can be made for the motion of spin density with charge density packet in two band model(electron, hole). Local deviation of charges from equilibrium cause a electric field defined by Poisson equation:

$$\nabla.\mathbf{E} = -\frac{e}{\epsilon}(\Delta n - \Delta p) \tag{2.1}$$

"$\Delta n = n - n_0$" and "$\Delta p = p - p_0$"; n, p and n_0, p_0 are the non-equilibrium and equilibrium densities of electron and hole respectively. Equation of continuity for electrons:

$$-\frac{\partial n}{\partial t} = -\nabla.\mathbf{j_e} - eG + eRnp \tag{2.2}$$

Where j_e is electron current, G and R are generation rate and recombination rate respectively. Inserting electron current from eq. (2.14) and using Poisson equation in above equation, assuming steady state condition and neglecting generation rate we get;

$$D_e \nabla^2 n - n\mu_e \nabla.\mathbf{E} + \mu_e \nabla n.E = \frac{n}{\tau_e} \tag{2.3}$$

similarly for hole:

$$D_h \nabla^2 n + n\mu_h \nabla.\mathbf{E} - \mu_h \nabla n.E = \frac{p}{\tau_h} \tag{2.4}$$

where $Rnp = \frac{n}{\tau_e} = \frac{p}{\tau_p}$, τ_e/τ_h is electron/hole flow rate, μ_e/μ_h is electron/hole mobility, D_e/D_h is electron/hole diffusion constant.

To establish single equation for electron and hole transportation with condition $\Delta n = \Delta p$ we get:

$$\sigma_h D_e \nabla^2 n + \sigma_e D_h \nabla^2 p + \sigma_h \mu_e \nabla n.\mathbf{E} - \sigma_e \mu_h \nabla p.\mathbf{E} = \frac{\sigma_h n}{\tau_e} + \frac{\sigma_e p}{\tau_h} \tag{2.5}$$

σ_e/σ_h is electron/hole conductivity, when $\Delta n \neq \Delta p$ then:

$$D_{ambi}\nabla^2 n + \mu_{ambi}\nabla n.\mathbf{E} = \frac{\Delta n}{\tau_r} \tag{2.6}$$

with $D_{ambi} = \frac{\sigma_h D_e + \sigma_e D_h}{\sigma_h + \sigma_e}$ is ambipolar diffusion constant and $\quad \mu_{ambi} = \frac{\sigma_h \mu_e - \sigma_e \mu_h}{\sigma_h + \sigma_e}, \quad \tau_r = \tau_e = \tau_h$ is ambipolar mobility.

Same approach can be done by inclusion of spin, but now we have four set of current equations. Two for electrons($\uparrow,\downarrow$) and two for holes($\uparrow,\downarrow$).

$$\mathbf{j_{e\uparrow\downarrow}} = \sigma_{e\uparrow\downarrow}\mathbf{E} + eD_{e\uparrow\downarrow}\nabla n_{\uparrow\downarrow} \tag{2.7}$$

Similarly equation of continuity by inclusion of spin can be written as,

Two equations for electron:

$$-e\frac{\partial n_{\uparrow(\downarrow)}}{\partial t} = -\nabla.\mathbf{j_{e\uparrow\downarrow}} \mp \frac{en_\downarrow}{\tau_{e\downarrow\uparrow}} \pm \frac{en_\uparrow}{\tau_{e\uparrow\downarrow}} - eG_{e\uparrow(\downarrow)} + eR_{\uparrow(\downarrow)\downarrow(\uparrow)}n_{\uparrow\downarrow}p_{\downarrow(\uparrow)} + eR_{\uparrow\uparrow(\downarrow\downarrow)}n_{\uparrow(\downarrow)}p_{\uparrow(\downarrow)} \tag{2.8}$$

Two equations for hole:

$$e\frac{\partial p_{\uparrow(\downarrow)}}{\partial t} = -\nabla.\mathbf{j_{h\uparrow\downarrow}} \pm \frac{ep_\downarrow}{\tau_{h\downarrow\uparrow}} \mp \frac{ep_\uparrow}{\tau_{h\uparrow\downarrow}} + eG_{e\uparrow(\downarrow)} - eR_{\downarrow(\uparrow)\uparrow(\downarrow)}n_{\downarrow\uparrow}p_{\uparrow(\downarrow)} - eR_{\uparrow\uparrow(\downarrow\downarrow)}n_{\uparrow(\downarrow)}p_{\uparrow(\downarrow)} \tag{2.9}$$

Now electric field produces within a system due to non-equilibrium distribution considering the spin given by Poisson's equation below:

$$\nabla.\mathbf{E} = -\frac{e}{\epsilon}(\Delta n_\uparrow + \Delta n_\downarrow - \Delta p_\uparrow - \Delta p_\downarrow) \tag{2.10}$$

Single equation which explain the transportation of carriers carrying spins:

$$D_s\nabla^2(n_\uparrow - n_\downarrow) + \mu_s\nabla(n_\uparrow - n_\downarrow).\mathbf{E} = \frac{\Delta n_\uparrow - \Delta n_\downarrow}{\tau_s} \tag{2.11}$$

Whereas diffusion constant D_s is modified with inclusion of spin and defined as:

$$D_s = \frac{\sigma_{e\uparrow} D_{e\downarrow} + \sigma_{e\downarrow} D_{e\uparrow}}{\sigma_{e\uparrow} + \sigma_{e\downarrow}}$$

And similarly mobility μ_s is:

$$\mu_s = \frac{\sigma_{e\uparrow} \mu_{e\downarrow} - \sigma_{e\downarrow} \mu_{e\uparrow}}{\sigma_{e\uparrow} + \sigma_{e\downarrow}}$$

Whereas $\tau_{e\downarrow\uparrow}$ and $\tau_{h\uparrow\downarrow}$ are the rate of spin relaxation for electrons and holes.

$$\tau_s^{-1} = \tau_{e\downarrow\uparrow}^{-1} + \tau_{h\uparrow\downarrow}^{-1}$$

Here we exclude the hole spin effect because very short life time. [13]

2.1.1 Spin transport and Conductivity:

Transportation of spin/charge describes that flow of electrons from higher concentration of spin/charge to low concentration. In material where the carrier density(CD) is high enough like in metals, small change in CD does not affect too much to conductivity. [14] In this situation it is easier to use to quasi-chemical potential equation to determine current flow:

$$\mathbf{j} = \sigma \nabla (\epsilon_\mu(r) - \phi(r)) \tag{2.12}$$

$$\mathbf{E} = \oint \mathbf{mc^2} \tag{2.13}$$

Where "σ" is conductivity and $\epsilon_\mu(\mathbf{r})$, $\phi(\mathbf{r})$ are the local chemical and electric potential respectively, whereas "$\epsilon_\mu(\mathbf{r}) - \phi(\mathbf{r})$" is the total chemical potential. For semiconductor where the CD is low enough, small change in density highly affect the conductivity. To measure current in such system by drift-diffusion equation:

$$\begin{aligned} \mathbf{j} &= \sigma\mathbf{E} + (\frac{\sigma k_\beta T}{n})\nabla \\ \mathbf{j} &= \sigma\mathbf{E} + eD\nabla n \end{aligned} \tag{2.14}$$

k_β is Boltzmann's constant E is electric field T is temperature n is carrier density, D is diffusion constant. spin dependent conductivity $\sigma_{\uparrow\downarrow}$ can be expressed:

$$\begin{pmatrix} \sigma_\uparrow \\ \sigma_\downarrow \end{pmatrix} = 0.5\sigma[1 + \beta\begin{pmatrix} 1 \\ -1 \end{pmatrix}] \tag{2.15}$$

whereas σ is effective conductivity β is spin selectivity. Spin $(\uparrow, \downarrow)$ electrons are in thermal equilibrium have different energies so they corresponds different bands. Diffusion of such electrons can be constructed by introduction of spin dependent chemical potential $\mu_{\uparrow\downarrow}$. Due to spin-orbit coupling two electron with different spin $(\uparrow, \downarrow)$ occupy different electronic state such splitting known as spin-split electronic structure. However the time reversal for two of momenta k will produce:

$$E_\uparrow(\mathbf{k}) = E_\downarrow(-\mathbf{k}) \tag{2.16}$$

where $E_{\uparrow\downarrow}(\mathbf{k})$ is the energy of spin-up $(\uparrow)$ and spin-down$(\downarrow)$ electron.

splitting of electronic structure is due to difference in the σ of $\uparrow$ and $\downarrow$; where as σ can be defined as

for degenerate:

$$\sigma_{\uparrow(\downarrow)} = n_{\uparrow(\downarrow)}e\mu_{\uparrow(\downarrow)} \tag{2.17}$$

for non-degenerate

$$\sigma_{\uparrow(\downarrow)} = N_{\uparrow(\downarrow)}(E_{\uparrow(\downarrow)})e^2 D_{\uparrow(\downarrow)} \tag{2.18}$$

21

Difference in mobility, diffusion constant and density of state are the cause of spin-split electronic structure. Spin current flow in magnetic material is due to difference in chemical potential, whereas in non-magnetic material it can be generated through spin-injection. in magnetic material due free electrons magnetic field remains always alive whereas in non-magnetic material it is due to motion of charges and vanishes by considering the spatial inversion symmetry along with time-reversal symmetry defined by eq.(2.16):

$$E_{\uparrow(\downarrow)}(\mathbf{k}) = E_{\uparrow(\downarrow)}(-\mathbf{k}) \tag{2.19}$$

2.2 Decoherence

Spin dynamics in materials would help to generate re-programable, non-volatile and quantum computation application. To introduce these one should know the spin coherence and transport properties. [15]

In semiconducting device like Op-Amp,P-N diode properties like rectification are controlled through the spatial motion of mobile carriers which are case sensitive to applied electric field or quasi-electric field, to coupled the spin to these mobile carriers generate new application. As spin of the carriers are quantized so resulting quantum coherence in these spin diminished when coupled to environment but for manipulation one need to coupled. So challenge is to manipulate spin to such extent that there is minimum decoherence. Spin system is characterized by two state system spin$\pm\frac{1}{2}$. Relative change in occupation and phase relationship is determined by the extent of perturbation. Spin relaxation times are denoted by t_1 and t_2 for longitudinal and transverse respectively, for single two state system t_1' is the relaxation time and t_2' is the coherence time. While considering the ensemble of spin then interaction between two state are permitted, and acquiring the information about single spin coherence and his life time lost. [16, 17]

Due to strong elastic magnetic dipolar interaction spins are aligned in a given state and time for which spin are remains coherent is defined as t_1'. Occupation imbalance causes a spin to relax to

lowest energy state due to spin lattice coupling and time required for this relaxation is defined as t_2'. Elastic dipolar interaction is always stronger then inelastic spin lattice interaction so $t_1' >> t_2'$ this effect is known as **Energy Bottleneck**.

For mobile electrons relaxation time and phase decoherence are approximately equal $t_1' \sim t_2'$, so there is no energy bottleneck. Spin-orbit coupling in materials the corresponding wave function can't be factorized into purely spin and orbital component, that's why spin eigenstates are called pseudospin eigen state.

Scattering-Driven Decoherence:- application of magnetic field causes a elastic scattering of electrons. Electrons lost their memory in other words they are not retraced at their previous positions, which cause a decoherence by elastic scattering. Either if there is no external stimuli (H=0), elastic scattering can be done by potential fluctuation.

Precessional Dephasing and Decoherence:- if the spin is oriented in $\hat{z}$ direction and homogeneous magnetic field (H) is applied in $\hat{x}$ the spin precess in yz-plan, and magnetization remains constant. In contrast when inhomogeneous (H(r)) is applied spin precess at different rate and angle, which causes dephasing of spin, when this dephasing such that previous position can't be retraced is known as decoherence. Average time τ is denoted for this lost of correlation between current location to previous one. There sre two regimes for Precessional Dephasing and Decoherence.

1. If the precessional frequency (Ω_p) is greater then transport of carriers then phasing angle spans $0 \rightarrow 2\pi$ before it lost correlation for complete decoherence. This regime leads to static inhomogeneous field leading to dephasing.

2. If transportation of carrier is greater then precessional frequency then decoherence occurs due to inhomogeneous field which is sum of static field(H_0) and time dependent spatial field($H(r)$) which changes after time τ. This fact is known as Motional narrowing.

Spatially inhomogeneous part of magnetic field varies with times τ also known as effective time for field reversal has $\partial H(r) = H(r) - H_0$, spin component which parallel to magnetization quantization of magnetic field axis '$S \cos(\Omega_\perp \tau)$' and transverse component '$S \sin(\Omega_\perp \tau)$'. $\Omega_\perp$ is the

precessional frequency can be thought of inhomogeneous part '$\Omega_\perp = g\mu\partial H(r)/\hbar$. If we consider the ensemble of spins then some precess about H_0 while other transported with spatially inhomogeneous part H_r, so there are randomness which cause decrement in fidelity. Somehow to find angle which spin make with quantization axis and decoherence time can be formulated by randomness of spins. Average length of the random walk made by spin is $\overline{[\Omega_\perp^2(r)]}^{1/2}\tau$ with step size T/τ, so average precession angle can be approximated as $\phi \sim \overline{[\Omega_\perp^2(r)\tau]}^{1/2}$ which leads to decoherence. Extent of decoherence determined by fractional change in spins with respect to spin quantization axis

$$\frac{\Delta S}{S} = 1 - \cos\phi = 1 - \cos([\Omega_\perp^2(r)\tau]^{1/2})$$

Using double angle formula $\cos 2\theta = 1 - 2\sin^2\theta$:

$$\frac{\Delta S}{S} = 1 - 1 + 2\sin([\Omega_\perp^2(r)\tau]/4) \tag{2.20}$$

Due to elastic dipolar interaction precession frequency (Ω) is small above equation can be modified;

$$\frac{\Delta S}{S} = [\Omega_\perp^2(r)\tau]/2 \tag{2.21}$$

This gives the measure of spins orientation relative to $H(r)$. For accurate spin manipulation needs measure of decoherence for direct band-gap materials precessional decoherence is prevailed. Such decoherence can be measured by the effect of time-dependent fluctuating field on electrons. This field exist even with no application of external magnetic field. Direction and magnitude of this field determine by crystal magnetic field which further can be calculated by crystal geometry. Timescale for such field are calculated through quasi-elastic orbital scattering which are due to neutral and ionized impurity, and optical phonon. Another source of decoherence is due to thermally unequilibrium population, diffusivity of carriers population also take place in decoherence. Free carriers can be divided into subpopulation and by quasi-elastic scattering decoherence time is same

in each subpopulation. Which can be written as:

$$\frac{1}{T_1} = \frac{1}{n} \int D(E)f(E)[1 - f(E)] \sum_l \tau_l(E)\Omega_l dE \tag{2.22}$$

'$D(E)$' is density of state, '$f(E)$' is probability of occupancy of given state, '$1 - f(E)$' is probability for empty state, 'n' is electrons density, '$\tau_l(E)$' is magnetic field reversal time and 'Ω_l' is precessional frequency for specific orbit. Field reversal time '$\tau_l(E)$' can be simulated by scattering cross section '$\sigma(\theta, E)$ for given orbital.

$$\tau_l^{-1} = \int_0^2 \pi\sigma(\theta, E)(1 - \cos[l\theta]d\theta \tag{2.23}$$

Monte Carlo method are used to determine the approximate numerical value '$\sigma(\theta, E)$. It can also determine by mobility;

$$\mu = \frac{e}{mn} \int D(E)f(E)[1 - f(E)]\tau_1(E)EdE \tag{2.24}$$

Carrier population is divided in '14' band model consist of '2' conduction anti-bonding 's' state (Γ_6), 6 valance (bonding) sate ($\Gamma_7 + \Gamma_8$) and 6 anti bonding 'p' state ($\Gamma_7 + \Gamma_8$).

2.3 Spin diffusion length 'l_s'

Spin diffusion length can be calculated from dielectric measurement with help of spin transport in material and drift diffusion equation. [18] Spin transport study gives the spin density helping for transport in material, while drift-diffusion equation helps us formulate spin diffusion length. spin dependent conductivity '$\sigma_{\uparrow\downarrow}$' can be expressed:

$$\begin{pmatrix} \sigma_\uparrow \\ \sigma_\downarrow \end{pmatrix} = 0.5\sigma[1 + \beta \begin{pmatrix} +1 \\ -1 \end{pmatrix}] \tag{2.25}$$

whereas 'σ' is effective conductivity 'β' is spin selectivity. Spin ($\uparrow, \downarrow$) electrons are in thermal equilibrium have different energies so they corresponds different bands. Number of spin-up and

spin-down electron in conduction band is;

$$\begin{pmatrix} n_\uparrow \\ n_\downarrow \end{pmatrix} = N_c e^{\frac{E_F - E_c}{kT}} \begin{pmatrix} e^{\frac{\mu_{spin}}{kT}} \\ e^{\frac{-\mu_{spin}}{kT}} \end{pmatrix} \tag{2.26}$$

'N_c' is the conduction electron, 'E_F' is the fermi energy of the material and 'μ_{spin}' is the chemical potential of spin-up and spin-down electrons at fermi level.

Spin dependent conductivity is defined as;

$$\begin{pmatrix} \sigma_\uparrow \\ \sigma_\downarrow \end{pmatrix} = e.(N_{Doping} + n_{accumul}).mobility.\begin{pmatrix} e^{\frac{\mu_{spin}}{kT}} \\ e^{\frac{-\mu_{spin}}{kT}} \end{pmatrix} \tag{2.27}$$

'N_{Doping}' is the number of doped atoms, '$n_{accumul}$' is the intrinsic accumulated density of atoms in conduction bands and 'e' is charge of electron. Effective conductivity '$\sigma = \sigma_\uparrow + \sigma_\downarrow$' which is sum of conductivity due to spin up and spin down electrons, which comes out to;

$$\sigma = e.(N_{Doping} + n_{accumul}).mobility.2.\cosh(\frac{\mu_{spin}}{kT}) \tag{2.28}$$

'σ' can be calculated from dielectric measurement of material (Experimental). So from above eq:2.28 'μ_{spin}' can be calculated;

$$\mu_{spin} = kT \cosh^{-1}\left[\frac{\sigma}{2e.(N_{Doping} + n_{accumul}).mobility}\right] \tag{2.29}$$

Spin selectivity 'β' is defined as;

$$\beta = \frac{\sigma_\uparrow - \sigma_\downarrow}{\sigma_\uparrow + \sigma_\downarrow} = \tanh(\frac{\mu_{spin}}{kT}) \tag{2.30}$$

Inserting eq:2.29 in eq:2.30 we get the 'β';

$$\beta = \tanh\left(\cosh^{-1}\left[\frac{\sigma}{2e.(N_{Doping} + n_{accumul}).mobility}\right]\right) \tag{2.31}$$

Spin diffusion length l_s depending on spin selectivity is defined as;

$$l_s = l_{s,0}\sqrt{1 - \beta^2} \tag{2.32}$$

Inserting eq:2.31 in eq:2.32 we will get spin diffusion length. Where $l_{s,0}$ is the intrinsic spin diffusion length.

2.4 Dielectric constant and Polarizability of materials

When material is placed in between parallel plates, charge (Q) on plates increases with biasing voltage (V) which can be written as;

$$Q = CV \tag{2.33}$$

Where 'C' is the capacitance offered by material. 'C' is also defined as the charge storing capacity of the material, and depends on material property dielectric constant' (ε), related as; $C = \varepsilon C_0$ where $C_0 = \frac{\varepsilon_0 A}{d}$ is the capacitance when the parallel plate capacitor is filled with vacuum and ε_0 defines the vacuum permittivity. Figure2.1 shows that dielectric material is placed in between
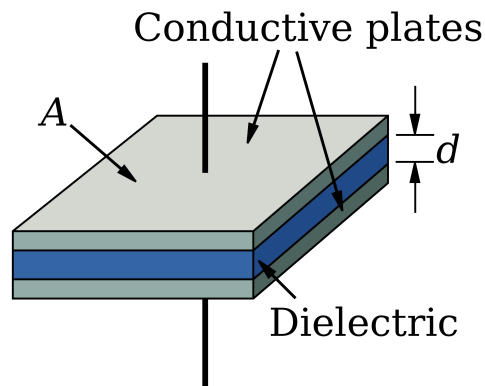
Figure 2.1: Dielectric is placed between two conducting plates, each of area 'A' and with a separation of 'd'.

conducting plate of area 'A' and separation between the plates is 'd', so capacitance 'C' is defined as $C = \frac{\varepsilon A}{d}$. [19]

2.4.1 Permittivity and Dielectric loss or tangent loss

Applied electric field causes electric displacement in material defined as;

$$D = \varepsilon E \tag{2.34}$$

$\varepsilon = \varepsilon_0 \varepsilon_r$ quantified the response of material with the iteration of applied electric field, whereas ε_r is the relative dielectric constant which vary from material to material. Complex dielectric is defined as:

$$\varepsilon = \varepsilon' - \iota \varepsilon'' \tag{2.35}$$

Where ε' is the real part of dielectric constant which shows the how much energy is stored in response to applied field and ε'' is the complex part of dielectric constant which is also known as dielectric loss shows the how much energy is dissipated to an external electric field. Its better to defined tangent loss for material which is defined as the ratio (or angle in a complex plane) of the lossy reaction to the electric field E in the curl equation to the lossless reaction:

$$\tan \delta = \frac{\varepsilon''}{\varepsilon'} \tag{2.36}$$

The relative "lossiness" of a material is the ratio of the energy lost to the energy stored. [20]

2.5 Polarization in material

When dielectric material is subjected to an electric field charge distribution in it get polarized according to the direction of applied electric field. Different type of polarization is observed which varies according to intensity of applied field.

2.5.1 Electronic polarization

When electric field is applied mostly electrons in the outer orbit shifted opposite to applied field. This phenomena occur so fast so no loss will be observed in dielectric constant. Slight shifting of electron is shown in figure 2.2.
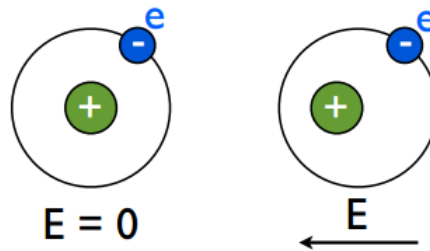
Figure 2.2: Electronic polarization without electric field $E = 0$ and with E.

2.5.2 Ionic Polarization

Ions are considered as charged masses connected to other charges by interatomic forces, when material is get polarized with the application of applied electric field ions are displaced from their position leaving the electronic cloud to other side. Which is another cause of polarization, variation of this polarization with the intensity of applied field is again constant because this phenomena occur so fast such that with in the regime of switching field. Slight shifting of ionic cloud is shown in figure 2.3.
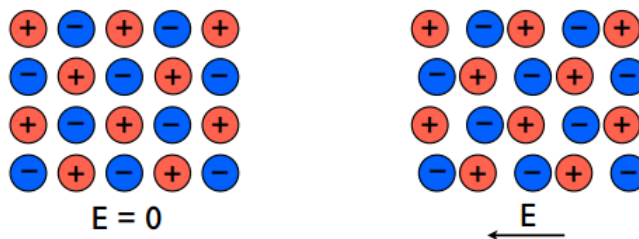
Figure 2.3: Ionic polarization without electric field $E = 0$ and with E.

2.5.3 Orientational polarization

Polarization can be defined in term of "dipole moment per unit volume", when electric field is applied dipole rotated according to applied field and try to aligned in the direction of applied field, this type of polarization caused a exponential decay in dielectric loss. Alignment of dipole moments with applied field are shown in figure 2.4.
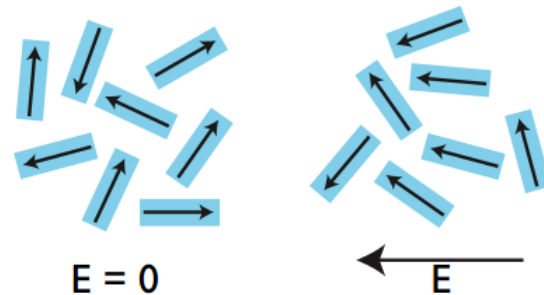
Figure 2.4: Orientational polarization without electric field $E = 0$ and with E.

2.5.4 Interfacial or space polarization

When material is multiphasic then charges accumulates at certain place and different regions are formed, those regions where charges accumulates are known as resistive regions and where from depleted known as capacitive region but overall capacitance in increased which is cause for increment in dielectric constant. Resistive and capacitive region is shown in figure 2.5.
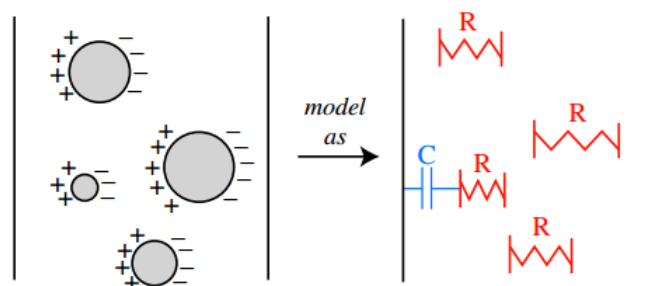
Figure 2.5: Interfacial or space polarization with applied field E.

2.5.5 Frequency dependance of polarization

Polarization in material changes with the frequency of applied, ionic and dipolar orientations are the weaker polarizations which are prominent at at low frequency (microwave), but as the frequency of applied field shifted to IR (infrared) region weaker contribution drops down. Only the stronger polarization act part which are atomic and electronic in dielectric constant. Change of dielectric constant with respect to different frequency is shown in figure 2.6.
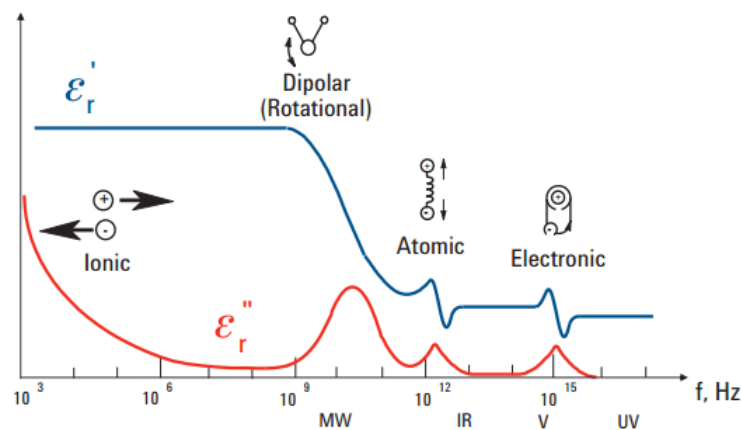
Figure 2.6: Frequency response of dielectric mechanisms.

2.6 Why ZnO?

Suitable choice of materials is needed to perform spintronics applications, as spin has to play prominent role. One way is to look at wide direct band gap semiconductor materials doped with transition metals. [21] These kind of hybrid structure known as dilute magnetic semiconductor (DMS) shows both charge plus spin manipulation, charge manipulation coming from inherent properties of semiconductor and spin transport property coming from dopant materials. But appropriate percentage and control environment is needed for doping of transition metals to avoid clustering and secondary phases. Recent research shows that non-metallic doping with low percentage shows room temperature (RT) ferromagnetism. [22] Which is primary requirement for spintronics devices. One of the wide band gap semiconductor material is ZnO, with incorporation

of carbon as dopant will have to show RT ferromagnetism. Different distinctive properties such Mechanical Properties, Dielectric, Vibrational Properties, Pyroelectricity, Spin Diffusion Length etc. are discussed below. [23, 24]

IIB and VIA compounds exhibit three kind of structures i) Zinc Blend ii) Wurtzite iii) Rock Salt, all have tetrahedral sp^3 covalent bonding. Among all these Wurtzite has thermodynamically stable structure, which can be obtain by two interpenetrating Hexagonal closed pack structure(HCP) along c-axis upto u=3/8=0.375. ZnO lies at borderline between ionic and covalent nature because due to ionizing character. Wurtzite structure $a \times b \times c \quad \langle 90^0 \times 90^0 \times 120^0 \rangle$ where a, b and c are lattice constant and values in Å.

Various theocratical calculation using Density Functional Theory (DFT) using Local Density Approximation (LDA) such as Linear Combination of Atomic Orbital (LCAO), Generalized Gradient Approximation (GGA), Hartree-Fock (HF),Hartree-Fock Perturbed Ion (HF-PI) etc. has been performed to investigate the different properties of ZnO. Property like total ground state energy calculated by assuming LCAO with first principle calculation using HF approximation [25, 25].

2.6.1 Lattice Parameter

Lattice parameter are affectively depends on free electrons concentration in conduction band, defects in crystal, environmental strain and temperature. Experimentally lattice parameter are determined using XRD-technique while theoretically calculation are also good agreement with experimental data, 'a, b' parameter ranges from 3.2475 to 3.2501Å where as 'c' ranges from 5.2042 to 5.2075Å. [26, 27]

2.6.2 Band structure

Experimentally band structure can be determined by using UV-Vis technique. Working principle of such technique based on scaling of energy needed for transition of electrons from valance band to conduction band. Theocratical calculation based on LDA by including the d electrons comes

out to be $E_g^{LDA} = 3.37eV$ which is closely related to experimental data for bandgap. [28]

2.6.3 Electrical Properties of ZnO

Advantages of large band gap of ZnO exhibits higher breakdown voltages, lower noise ratio, high power operation, higher melting temperature and ability to sustain large electric field. At lower electric field energy gained is comparatively less then the thermal agitation, so there is no effect in energy distribution of electrons. But at higher electric field energy distribution is effected from equilibrium point. Hall effect is most widely used for measurement of electric transport properties, where as theocratically Monte Carlo simulation are used to study the transport properties. For ZnO $\sim 17cm^2/(Vs)$ mobility is measured with carrier concentration of $\sim 10^6 cm^{-1}$. [29]

2.6.4 Carbon-doped ZnO

Electronic configuration of Zn atom is $[Ar]3d^{10}4s^2$ and for oxygen atoms $1s^22s^22p^4$, +2 oxidation state of Zn atoms forms sp^3 covalent bonding with four nearest neighbors of oxygen atoms. Due to having ionicity upto greater extent ZnO have substantial ionic character. Electronic configuration for Carbon atom is $[He]2s^22p^2$, it will disturb the sp^3 hybridization when it is doped. There are two lattice sites where carbon can reside first at Zn site which is hardly to occur because Zn atom is screened by four oxygen atoms other reason is that it is 5 times less then the atomic mass of Zn. In others words carbon atom has not enough momentum to replace Zn atoms. Second lattice site is oxygen site, where it can reside due to almost same atomic size. Substitution of C at oxygen lattice site also responsible for room temperature ferromagnetism (RTF). A strong coupling between carbon 2p and Zn 4s,3d, due to exchange interaction spin spilt state are formed. There is p-p exchange interaction in localized C2p and valance band electrons, these interaction carries magnetism along with due to large contribution by magnetic moments. And there is also small contribution by neighbouring Zn atoms and second nearest O atoms. For doping principle dopant material can alter the chemical and physical properties retaining the crystal structure same. [30]

2.7 Relation between electrical and dielectric properties

UV-Vis is commonly known as electronic absorption spectrum, energy required to excite the electrons from initial state ψ_i to final state ψ_f is of ultraviolet and visible region of electromagnetic spectrum. [31] The change in intensity of incident wave can be described by Beer's Law as below:

$$
\begin{aligned}
dI &= -\alpha dx \times I(x) \\
I(x) &= I_0 e^{-\alpha x}
\end{aligned}
\tag{2.37}
$$

Here α is absorption coefficient of material and x is length of material through which radiation passes and I_0 is intensity defined at x=0. And corresponding transition probability can be determined by matrix element $< \psi_i|\mu.\mathbf{E}|\psi >$, where μ is electric dipole moment and $\mathbf{E}$ is applied electric field. For multiple transition density of state are to considered. Now considering the plane wave of the incident electric field:

$$
\mathbf{E}(\mathbf{x}, \mathbf{t}) = \mathbf{E_0} e^{i(\mathbf{k}\mathbf{x} - wt)}
\tag{2.38}
$$

Propagation vector $\mathbf{k}$ can be defined as $k = \frac{2\pi}{\lambda} = \frac{n\omega}{c}$. In non-absorbing medium wavelength is reduced by refractive index of material (λ/n) through which wave is propagating. For absorbing materials refractive index is sum of real and complex part and defined by $\tilde{n} = n + ik_{ex}$, where k_{ex} is extinction coefficient. So modified propagation vector:

$$
\mathbf{k} = (n + ik_{ex})\frac{\omega}{c}
\tag{2.39}
$$

Inserting in eq:2.38 to defined the electric field in absorbing materials we get:

$$
\mathbf{E}(\mathbf{x}, \mathbf{t}) = \mathbf{E_0} e^{\frac{kx\omega}{c}} e^{i(\frac{\omega nx}{c} - wt)}
\tag{2.40}
$$

Corresponding intensity is defined as $I = \frac{\sigma E^2(x,t)}{\sigma E^2(0)}$, here σ is conductivity of material and consider to be uniform through out the system.

$$
\begin{aligned}
E^2(x,t) &= E(x,t)E^*(x,t) \\
E^2(x,t) &= E_0^2 e^{-\frac{2k_{ex}\omega x}{c}} \\
I = \frac{E^2(x,t)}{E_0^2} &= e^{-\frac{2k_{ex}\omega x}{c}}
\end{aligned}
\tag{2.41}
$$

Compering with eq:2.37 we get absorption coefficient α:

$$
\alpha = \frac{2k_{ex}\omega}{c} = \frac{4\pi k_{ex}}{\lambda}
\tag{2.42}
$$

Here one can say that absorption is directly related to extinction coefficient. Extinction can be derived from relative dielectric constant (ϵ_r), the relationship between relative dielectric constant and refractive index can be derived from Maxwell's equations which is $n^2 = \epsilon_r$. Analogy with complex refractive index the complex relative dielectric constant can be defined below:

$$
\tilde{\epsilon}_r = \epsilon_1 + i\epsilon_2
\tag{2.43}
$$

Where ϵ_1 and ϵ_2 are the real and complex part of relative dielectric constant respectively. After solving having the analogy $\tilde{n}^2 = \tilde{\epsilon}_r$ we get:

$$
\begin{aligned}
\epsilon_1 &= n^2 - k_{ex}^2 \tag{2.44} \\
\epsilon_2 &= 2nk_{ex} \tag{2.45}
\end{aligned}
$$

Where

$$
n = \sqrt{\frac{\epsilon_1 + (\epsilon_1^2 + \epsilon_2^2)^{\frac{1}{2}}}{2}} \quad , \quad k_{ex} = \sqrt{\frac{-\epsilon_1 + (\epsilon_1^2 + \epsilon_2^2)^{\frac{1}{2}}}{2}}
$$

From previous couple of equations we can conclude that 'n' and 'ϵ' are not independent.

There is another way to find absorption coefficient if length of solution to which incident wave

propagate and concentration of solution are known. Absorbance are defined:

$$
\begin{aligned}
A &= \log \frac{I(x)}{I_0} \\
&= \varepsilon x c = \alpha c
\end{aligned}
\tag{2.46}
$$

'ε' is molar absorptivity, x is the length of solution for solids this is just the dimensions and c is the concentration.

Chapter 3

Nucleation, Synthesis and characterizations for ZnO and C-doped ZnO nanowires

When particles agglomerate to form crystal, interface is created due to difference in chemical potential and surface energy of respective phases. Interfacial energy creates barrier which stop further particles from self diffusion, this barrier can be adjusted by controlling the thermodynamic variables. With the help of interfacial energy total energy (Gibs Energy) can be formulated, further nucleation rate can be estimated. As difference in surface area exposed to nucleation for 0-dimensional, 1-dimensional and 2-dimensional where particles have n+1 degree of freedom, there is difference in interfacial profile hence nucleation rate for different dimensional structure can estimated.

3.1   Introduction

In supersaturated solution molecular addition of particles forms clusters, further addition to these cluster cause growth of crystal structure, this process is known as nucleation. Particle size and its

solubility can be seen in Gibbs-Thomson relation:

$$\ln\left[\frac{c(L)}{c}\right] = \frac{2VF\sigma_{\alpha\beta}}{3k_\beta TL} \tag{3.1}$$

"$c(L)$" is solubility of crystal as function of diameter or length(L) of side coupled with shape factor "F", "c" is the solubility of substance at equilibrium, "k_β" is boltzman constant,σ_{LV} is interfacial energy between liquid and solid phases and "V" is the molecular volume. Ratio of "$c(L)$" to "c" gives degree of supersaturation (S). High concentration of particles in supersaturated or super-cooled solution nucleates to form bigger particles and this growth is in different directions [32] [33]After reaching a critical radius in nucleation process further growth cause a bigger particle which is highly unstable, so to nucleate a different structure controlled environment is required. Growth mechanism and nucleation of nano-particle described by LaMer Brust nucleation. [34] And size of particle described by Ostwald ripening. Homogeneous nucleation can be described by total free energy available which is sum of surface free energy and volume free energy of system.

$$\Delta G = 4\pi r^2 \sigma_{\alpha\beta} + \frac{4}{3}\pi r^3 \Delta G_V \tag{3.2}$$

where r is the radius, $\sigma_{\alpha\beta}(j.m^{-2})$ is the interfacial energy between two phases and $\Delta G_V(j.m^{-3})$ is the negative free enthalpy change. Applying maximization$\frac{\partial \Delta G}{\partial r} = 0$ condition to find critical energy ΔG_c needed for nucleation to start which results:

$$\Delta G_c = \frac{16\pi\sigma_{\alpha\beta}^3}{3\Delta G_V^2} \quad \text{with,} \quad r_c = -\frac{2\sigma_{\alpha\beta}}{\Delta G_V} \tag{3.3}$$

orΔG_c can be written in term of critical radius as:

$$\Delta G_c = \frac{4}{3}\pi\sigma_{\alpha\beta}^2 r_c^2 \tag{3.4}$$

Based on critical energy or barrier energy needed to start nucleation,In 1926 Volmer and Weber formulated a nucleation rate "j" ($s^{-1}.m^{-3}$) in which they assumed frequency per unit volume of nucleus formed is proportional to critical nuclei population. [35] Further Nucleation rate was

improvised by Becker & Doring and then Turnbull and Fisher proposed the nucleation rate as: [36]

$$j = K(T) \exp(\frac{-\Delta G_c}{k_\beta T}) \tag{3.5}$$

where k_β is Boltzman constant and $K(T)$ is pre-exponent constant which is function of temperature can be defined by:

$$K(T) = n^* N_o v(\frac{r_c^2 \sigma_{\alpha\beta}}{\Delta G_c k_\beta T}) \tag{3.6}$$

n^* is the number of surface atom across nucleus,N_o is the number density and v is vibrational frequency. $K(T)$ is one parameter which distinguish between homogeneous and heterogeneous nucleation, it can been determined experimentally by considering the effect of sample volume on nucleation rate. For liquid *Hg* drop its value comes out to be $10^{39\pm1}(s^{-1}.m^{-3})$. [37]

From eq.(3.1)we can defined:

$$-\Delta G_V = \frac{2\sigma_{\alpha\beta}}{3L} = \frac{k_\beta T \ln S}{VF} \tag{3.7}$$

Putting eq.(3.7)in (3.3) we get ΔG_c in term of degree of supersaturation:

$$\Delta G_c = \frac{16\pi \sigma_{\alpha\beta}^3 V^2 F^2}{3(k_\beta T \ln S)^2} \tag{3.8}$$

Hence the nucleation rate can be defined:

$$j = K(T) \exp(\frac{-16\pi \sigma_{\alpha\beta}^3 V^2 F^2}{3k_\beta^3 T^3 (\ln S)^2}) \tag{3.9}$$

3.2 Interfacial energy

If we have binary system(α, β) different in chemical potential then total free energy of system is function of composition and composition gradient can be defined as $f(c, \nabla c, \nabla^2 c)$, applying taylor

series we get:

$$f(c, \nabla c, \nabla^2 c) = f_o(c) + \sum_i L_i(\frac{\partial c}{\partial x_i}) + \sum_{ij} k_{ij}^{(1)}(\frac{\partial^2 c}{\partial x_i \partial x_j}) + \frac{1}{2}\sum_{ij} k_{ij}^{(2)}[(\frac{\partial c}{\partial x_i})(\frac{\partial c}{\partial x_j})] + ...(3.10)$$

where; $L_i = [\partial f/\partial(\frac{\partial c}{\partial x_i})]$; $\quad k_{ij}^{(1)} = [\partial f/\partial(\frac{\partial^2 c}{\partial x_i \partial x_j})]$ $\quad$ and $\quad k_{ij}^{(2)} = [\partial^2 f/\partial(\frac{\partial c}{\partial x_i})\partial(\frac{\partial c}{\partial x_j})]$

And $f_0(c)$ free energy density defined by Helmholtz function (F)

$$f_0(c) = \frac{F}{N_a} = \frac{\Delta E - TS}{N_a} \tag{3.11}$$

E and S is Internal energy and Entropy of the system respectively and "$N_a = N_\alpha + N_\beta$" is the total number of atoms. Applying the constraint such as reflection $(i \to -i)$ and rotation $(i \to j)$ to free energy available of system therefore:

$$L_i = 0, \quad k_{ij}^{(1)} = k_1 = \left[\frac{\partial f}{\partial \nabla^2 c}\right]_0 \quad with \quad i = j \quad k_1 = 0 \quad for \quad i \neq j \tag{3.12}$$

$$k_{ij}^{(2)} = k_2 = \left[\frac{\partial^2 f}{(\partial \nabla c)^2}\right]_0 \quad with \quad i = j \quad k_2 = 0 \quad for \quad i \neq j \tag{3.13}$$

So eq:(3.10) can be written as:

$$f(c, \nabla c, \nabla^2 c) = f_o(c) + k_1 \nabla^2 c + \frac{1}{2}k_2(\nabla c)^2 + ... \tag{3.14}$$

Integrating over volume and applying boundary condition $\nabla c.n = 0$ the total energy of the system becomes and :

$$F = N_V \int_V [f_o(c) + k(\nabla c)^2 + ...]dV \tag{3.15}$$

Where $k = -\frac{dk}{dc} + \frac{1}{2}k_2$, inserting values of k_1 and k_2 from eq: (3.12) and (3.13)

$$k = -\frac{d}{dc}[\frac{\partial f}{\partial \nabla^2 c}]_0 + \frac{1}{2}[\frac{\partial^2 f}{(\partial \nabla c)^2}]_0 \tag{3.16}$$

Considering the gradient of composition in one direction eq.(3.15 becomes:

$$F = AN_V \int_{-\infty}^{+\infty} [f_o(c) + k(\frac{dc}{dx})^2] dx \tag{3.17}$$

Chemical potential "μ" can be determined by taking derivative of total free energy "F" with respect to concentration of solution:

$$\mu = \frac{\partial F}{\partial c} = f'_0(c) - 2k\frac{\partial c}{\partial x} \tag{3.18}$$

Interfacial energy(total free energy per unit area)$\sigma_{\alpha\beta}$ is defined as difference between free energy of system and chemical potential of respective phases:

$$\sigma_{\alpha\beta} = \frac{F}{A} = N_V \int_{-\infty}^{+\infty} [\{f_o(c) + k(\frac{dc}{dx})^2\} - \{c\mu_\beta(e) + (1-c)\mu_\alpha(e)\}] dx \tag{3.19}$$

Where $\mu_\beta(e)$ and $\mu_\alpha(e)$ are the chemical potential of α and β phases. Simplifying (3.19) we get:

$$\sigma_{\alpha\beta} = N_V \int_{-\infty}^{+\infty} [\Delta f(c) + k(\frac{dc}{dx})^2] dx \tag{3.20}$$

where

$$\Delta f(c) = f_o(c) - \{c\mu_\beta(e) + (1-c)\mu_\alpha(e)\} \tag{3.21}$$

Stationary values of intergradient in eq.(3.20) can be achieved by using Euler equation. For minimum values $\Delta f(c) = k(\nabla c)^2$ and changing variable for $x \to c$ it becomes:

$$\sigma_{\alpha\beta} = 2N_V \int_{c_\alpha}^{c_\beta} [k\Delta f(c)]^{\frac{1}{2}} dc \tag{3.22}$$

Eq.(3.22) described the dependence of $\sigma_{\alpha\beta}$ on composition profile of system.

Temperature dependency on interfacial energy can be obtained by considering the conjugate tem-

perature T_c(where two phases attain the same critical composition (c_c)).

$$\Delta f_{(T \sim T_c)} = -\beta(T_c - T)[(\Delta c)^2 - (\Delta c_c)^2] + \gamma[(\Delta c)^4 - (\Delta c_c)^4] + ... \quad (3.23)$$

Above equation is obtained by applying Taylor enpension on eq.(3.21)around $f_c(c)$ where:

$$\Delta c = c - c_c \quad \Delta c_c = c_\beta - c_c = c_c - c_\alpha \quad (3.24)$$

$$\beta = \frac{(\partial^3 f_0/\partial T \partial c^2)}{2!} \quad (3.25)$$

$$\gamma = \frac{(\partial^4 f_0/\partial c^4)}{4!} \quad (3.26)$$

Now interfacial energy can written after doing some mathematical steps:

$$\sigma_{\alpha\beta(T \sim T_c)} = 2N_V \int_{-\Delta c_e}^{+\Delta c_e} (k\gamma)^{\frac{1}{2}}[(\Delta c_e)^2 - (\Delta c)^2]d(\Delta c) \quad (3.27)$$

Applying mean value theorem to above equation interfacial energy becomes:

$$\sigma_{\alpha\beta(T \sim T_c)} = (\frac{2\sqrt{2}N_V}{3\gamma})k^{\frac{1}{2}}\beta^{\frac{3}{2}}(T_c - T)^{\frac{3}{2}} \quad (3.28)$$

Helmholtz function before mixing of binary homogeneous system is; $F^0 = E^0 - TS^0 = (1 - c)F_\alpha^0 + cF_\beta^0$ and after mixing is defined as; $F_{mix} = F^0 + \Delta F_{mix}$, whereas ΔF_{mix} is molar Halmholtz energy of mixing and it's equal to $\Delta F_{mix} = \Delta E_{mix} - T\Delta S_{mix}$. ΔS_{mix} is the entropy after mixing and it can be defined by Boltzman eq.$\Delta S_{mix} = k \ln \frac{W_{mix}}{W^0}$, W^0 and W_{mix} are number of ways in which the N_α and N_β can be arranged before and after mixing.$W^0 = 0$ for indistinguishable state. And $W_{mix} = \frac{N_a!}{N_\alpha! N_\beta!} = \frac{N_\alpha! + N_\beta!}{N_\alpha! N_\beta!}$, so;

$$\Delta S_{mix} = k \ln \frac{N_a!}{N_\alpha! N_\beta!} \quad (3.29)$$

Applying Stirling formula $\ln N! \approx N \ln N - N$ to above eq. we get:

$$\Delta S_{mix} = -R[(1 - c) \ln(1 - c) + c \ln c] \quad (3.30)$$

whereas $R = kN_a$. To find internal energy change ΔE_{mix} in binary system after mixing we have to calculate E_{mix} as the pairwise sum of interatomic potentials $(\varepsilon_{\alpha\alpha}, \varepsilon_{\beta\beta}, \varepsilon_{\alpha\beta})$ for each atom in the solution.

$$E = P_{\alpha\alpha}\varepsilon_{\alpha\alpha} + P_{\beta\beta}\varepsilon_{\beta\beta} + P_{\alpha\beta}[\varepsilon_{\alpha\beta} - \frac{1}{2}(\varepsilon_{\alpha\alpha} + \varepsilon_{\beta\beta})] \tag{3.31}$$

Whereas $P_{\alpha\alpha}, P_{\beta\beta}, P_{\alpha\beta}$ are the number bonds between in solution. And can be determined by probabilistic way on the basis of nearest neighbours "z".

$$P_{\alpha\alpha} = \frac{N_\alpha z}{2} - \frac{P_{\alpha\beta}}{2}; \quad P_{\beta\beta} = \frac{N_\beta z}{2} - \frac{P_{\alpha\beta}}{2} \quad and \quad P_{\alpha\beta} = zN_a c(1-c) \tag{3.32}$$

$N_\alpha,\quad N_\beta,\quad and\quad N_a = N_\alpha + N_\beta$ are number of nearest belabours atoms in respective phases. In eq.(3.31)first two terms on right side are the intrinsic contributions to internal energy, and third term due to mixing, so change in internal energy can be determined by:

$$\begin{aligned} \Delta E_{mix} &= E - [P_{\alpha\alpha}\varepsilon_{\alpha\alpha} + P_{\beta\beta}\varepsilon_{\beta\beta}] = P_{\alpha\beta}[\varepsilon_{\alpha\beta} - \frac{1}{2}(\varepsilon_{\alpha\alpha} + \varepsilon_{\beta\beta})] \\ \Delta E_{mix} &= \Omega c(1-c) \end{aligned} \tag{3.33}$$

Where $\Omega = zN_a[\varepsilon_{\alpha\beta} - \frac{1}{2}(\varepsilon_{\alpha\alpha} + \varepsilon_{\beta\beta})]$ is regular solution constant.

3.3   Results

Inserting equations(3.30) and (3.33) in the (3.11) to find the "$f_0(c)$" free energy density:

$$f_0(c) = \frac{1}{N_a}[\Omega c(1-c) + RT\{(1-c)\ln(1-c) + c\ln c\}] \tag{3.34}$$

Conjugate temperature can be defined as $T_c = \frac{\Omega}{2R}$.

$$T_c = \frac{zN_a[\varepsilon_{\alpha\beta} - \frac{1}{2}(\varepsilon_{\alpha\alpha} + \varepsilon_{\beta\beta})]}{2R} \tag{3.35}$$

By putting $f_0(c)$ in eq.(3.25) and(3.26) we got the values of β and γ as follows:

$$\beta = \frac{R}{2N_a}[\frac{1}{1-c} + \frac{1}{c}] \tag{3.36}$$

$$\gamma = \frac{RT}{12N_a}[\frac{1}{(1-c)^3} + \frac{1}{c^3}] \tag{3.37}$$

3.3.1   0-dimensional structure

Considering the spherical particle with concentration "$c = \frac{4}{3}\pi r^3 = ar^3$" and it's distributed spherical symmetrical the value of "k" can be determined by solving eq.(3.16).

$$\begin{aligned}
k &= -\delta c^{\frac{-1}{3}}[\frac{1}{12}\{\Omega(7-8c) + RT(\ln(\frac{c}{1-c})^7 - 3(\frac{1-2c}{1-c}))\} \\
&\quad + ca^{\frac{1}{6}}\{-2\Omega + RT(\frac{1}{c(1-c)})\}]
\end{aligned} \tag{3.38}$$

where "$\delta = \frac{1}{2a^{\frac{2}{3}}N_a}$".

Now interfacial energy can be calculated by inserting equations (3.35),(3.36),(3.37) and (3.38 in (3.28) we get:

$$\begin{aligned}
\sigma_{\alpha\beta(T\sim T_c)} &= [2\sqrt{2}N_V/\frac{RT}{4N_a}\{\frac{1}{(1-c)^3} + \frac{1}{c^3}\}][-\delta c^{\frac{-1}{3}}\{\frac{1}{12}(\Omega(7-8c) + RT(\ln(\frac{c}{1-c})^7 - \frac{3-6c}{1-c}))\} \\
&\quad + ca^{\frac{1}{6}}\{-2\Omega + \frac{RT}{c(1-c)}\}]^{\frac{1}{2}}[\frac{R}{2N_a}(\frac{1}{1-c} + \frac{1}{c})]^{\frac{3}{2}}[\frac{zN_a(2\varepsilon_{\alpha\beta} - \varepsilon_{\alpha\alpha} - \varepsilon_{\beta\beta})}{4R} - T]^{\frac{3}{2}} \quad (3.39)
\end{aligned}$$

Inserting above expression for interfacial energy in eq.(3.9) to find the nucleation rate for spherical shape particles.

3.3.2   1-dimensional structure

Considering the cylindrical shape with concentration "$c = \pi r^2 z$" where "z" is length of cylinder. Any by using cylindrical coordinate we can find gradient in concentration "$\delta c = \frac{\partial c}{\partial r}\hat{r} + \frac{1}{r}\frac{\partial c}{\partial \phi}\hat{\phi} +$

$\frac{\partial c}{\partial z}\hat{z}$".By using eq.(3.16) value of "k" can be determined which comes out:

$$
\begin{aligned}
k &= -\frac{1}{N_a 4\pi}[\{\frac{\Omega}{z}(1-4c) + \frac{RT}{z}(\ln\frac{c}{1-c} + \frac{1}{1-c})\} - \{\frac{4\Omega z}{4z^2+1}(1-6c) \\
&\quad + \frac{4zRT}{4z^2+1}(\ln\frac{c}{1-c} + \frac{2}{1-c}) + \frac{\Omega}{z}(1-6c) + 2\pi RT(\ln\frac{c}{1-c} + \frac{2}{1-c}) \\
&\quad + 2\Omega(\frac{-z^4 - 4z^2 + cz - c}{z(4z^2+1)}) - \frac{2RTz^3}{4z^2+1}(\ln\frac{c}{1-c} + \frac{1}{z(1-c)}) \\
&\quad + \Omega(\frac{-z^4 + 2z^3 - 4z^2 - c}{4z^3}) + RT(\frac{-z}{4}\ln\frac{c}{1-c} + \frac{\pi}{z(1-c)})\}]
\end{aligned}
\tag{3.40}
$$

Now interfacial energy for cylindrical shape can be calculated by inserting equations (3.35),(3.36),(3.37) and (3.40 in (3.28) we get:

$$
\begin{aligned}
\sigma_{\alpha\beta(T\sim T_c)} &= [2\sqrt{2}N_V / \frac{RT}{4N_a}\{\frac{1}{(1-c)^3} + \frac{1}{c^3}\}][-\frac{1}{N_a 4\pi}[\{\frac{\Omega}{z}(1-4c) + \frac{RT}{z}(\ln\frac{c}{1-c} \\
&\quad + \frac{1}{1-c})\} - \{\frac{4\Omega z}{4z^2+1}(1-6c) + \frac{4zRT}{4z^2+1}(\ln\frac{c}{1-c} + \frac{2}{1-c}) + \frac{\Omega}{z}(1-6c) \\
&\quad + 2\pi RT(\ln\frac{c}{1-c} + \frac{2}{1-c}) + 2\Omega(\frac{-z^4 - 4z^2 + cz - c}{z(4z^2+1)}) - \frac{2RTz^3}{4z^2+1}(\ln\frac{c}{1-c} \\
&\quad + \frac{1}{z(1-c)}) + \Omega(\frac{-z^4 + 2z^3 - 4z^2 - c}{4z^3}) + RT(\frac{-z}{4}\ln\frac{c}{1-c} \\
&\quad + \frac{\pi}{z(1-c)})\}]^{\frac{1}{2}}[\frac{R}{2N_a}(\frac{1}{1-c} + \frac{1}{c})]^{\frac{3}{2}}[\frac{zN_a(2\varepsilon_{\alpha\beta} - \varepsilon_{\alpha\alpha} - \varepsilon_{\beta\beta})}{4R} - T]^{\frac{3}{2}}
\end{aligned}
\tag{3.41}
$$

Inserting above expression in eq.(3.9) to find the nucleation rate for cylindrical shapes.

3.3.3 2-dimensional structure

We considering the concentration is "$c = xyz$" is distributed along surfaces,where x-length, y-width, z-height.

$$
\begin{aligned}
\nabla c &= \frac{\partial c}{\partial x}\hat{x} + \frac{\partial c}{\partial y}\hat{y} + \frac{\partial c}{\partial z}\hat{z} = yz\hat{x} + xz\hat{y} + xy\hat{z} \\
|\nabla c| &= \sqrt{(yz)^2 + (xz)^2 + (xy)^2} \quad \text{and} \quad \nabla^2 c = 0
\end{aligned}
\tag{3.42}
$$

Eq. (3.16) can be re-written for 2-dimensional structure:

$$k \quad = \quad \frac{1}{2}\left[\frac{\partial^2 f}{(\partial \nabla c)^2}\right]_0 \tag{3.43}$$

where

$$\frac{\partial^2 f_0}{\partial|\nabla c|^2} \quad = \quad \frac{\partial}{\partial|\nabla c|}\left(\frac{\partial f_0}{\partial|\nabla c|}\right) = \frac{\partial}{\partial|\nabla c|}\left(\frac{\partial f_0}{\partial x}\frac{\partial x}{\partial|\nabla c|} + \frac{\partial f_0}{\partial y}\frac{\partial y}{\partial|\nabla c|} + \frac{\partial f_0}{\partial z}\frac{\partial z}{\partial|\nabla c|}\right) \tag{3.44}$$

f_0 is defined by eq.(3.34). After solving above equation we get:

$$\begin{aligned}
\frac{\partial^2 f_0}{\partial|\nabla c|^2} \quad = \quad & \frac{1}{N_a}\frac{\partial}{\partial|\nabla c|}[(\Omega yz(1-2xyz) + RTyz\ln\frac{xyz}{1-xyz}).\frac{|\nabla c|}{x(z^2+y^2)} \\
& +(\Omega xz(1-2xyz) + RTxz\ln\frac{xyz}{1-xyz}).\frac{|\nabla c|}{y(z^2+x^2)} \\
& +(\Omega xz(1-2xyz) + RTxy\ln\frac{xyz}{1-xyz}).\frac{|\nabla c|}{z(x^2+y^2)}]
\end{aligned} \tag{3.45}$$

Equivalently we can write:

$$\frac{\partial^2 f_0}{\partial|\nabla c|^2} = \frac{1}{N_a}\frac{\partial}{\partial|\nabla c|}[f_1(x,y,z) + f_2(x,y,z) + f_3(x,y,z)] \tag{3.46}$$

Where

$$\frac{\partial f_1}{\partial|\nabla c|} = [\frac{\partial f_1}{\partial x}\frac{\partial x}{\partial|\nabla c|} + \frac{\partial f_1}{\partial y}\frac{\partial y}{\partial|\nabla c|} + \frac{\partial f_1}{\partial z}\frac{\partial z}{\partial|\nabla c|}] \tag{3.47}$$

$$\frac{\partial f_2}{\partial|\nabla c|} = [\frac{\partial f_2}{\partial x}\frac{\partial x}{\partial|\nabla c|} + \frac{\partial f_2}{\partial y}\frac{\partial y}{\partial|\nabla c|} + \frac{\partial f_2}{\partial z}\frac{\partial z}{\partial|\nabla c|}] \tag{3.48}$$

$$\frac{\partial f_3}{\partial|\nabla c|} = [\frac{\partial f_3}{\partial x}\frac{\partial x}{\partial|\nabla c|} + \frac{\partial f_3}{\partial y}\frac{\partial y}{\partial|\nabla c|} + \frac{\partial f_3}{\partial z}\frac{\partial z}{\partial|\nabla c|}] \tag{3.49}$$

After solving we get:

$$\frac{\partial f_1}{\partial |\nabla c|} = [\{(-\frac{2\Omega c^2}{x^2} + RT[\frac{c}{x^2} + \frac{c^2}{x^2(1-c)}])(\frac{|\nabla c|^2}{x^2(z^2+y^2)^2}) + (\frac{\Omega c}{x}(1-2c)$$

$$+RT[\frac{c}{x}\ln\frac{c}{1-c}])(\frac{1}{x(z^2+y^2)} - \frac{|\nabla c|^2}{x^3(z^2+y^2)^2})\} + \{(\Omega z(1-4c)$$

$$+RT[z\ln\frac{c}{1-c} + z + \frac{cz}{1-c}])(\frac{|\nabla c|^2}{xy(z^2+y^2)(z^2+x^2)}) + (\frac{\Omega c}{x}(1-2c)$$

$$+RT[\frac{c}{x}\ln\frac{c}{1-c}])(\frac{1}{x(z^2+y^2)} - \frac{2|\nabla c|^2}{x(x^2+y^2)(z^2+x^2)})\} + \{(\Omega y(1-4c)$$

$$+RT[y\ln\frac{c}{1-c} + y + \frac{cy}{1-c}])(\frac{|\nabla c|^2}{xz(z^2+y^2)(y^2+x^2)}) + (\frac{\Omega c}{x}(1-2c)$$

$$+RT[\frac{c}{x}\ln\frac{c}{1-c}])(\frac{1}{x(z^2+y^2)} - \frac{2|\nabla c|^2}{x(z^2+y^2)^2(x^2+y^2)})\}] \tag{3.50}$$

and

$$\frac{\partial f_2}{\partial |\nabla c|} = [\{(\Omega z(1-4c) + RT[z\ln\frac{c}{1-c} + z + \frac{cz}{1-c}])(\frac{|\nabla c|^2}{xy(z^2+x^2)(z^2+y^2)}) + (\Omega\frac{c}{y}(1-2c)$$

$$+RT[\frac{c}{y}\ln\frac{c}{1-c}])(\frac{1}{y(z^2+x^2)} - \frac{2|\nabla c|^2}{y(z^2+x^2)^2(z^2+y^2)})\} + \{(-\frac{2\Omega c^2}{y^2}$$

$$+RT[\frac{c}{y^2} + \frac{c^2}{y^2(1-c)}])(\frac{|\nabla c|^2}{y^2(z^2+x^2)^2}) + (\Omega\frac{c}{y}(1-2c)$$

$$+RT[\frac{c}{y}\ln\frac{c}{1-c}])(\frac{1}{y(z^2+x^2)} - \frac{|\nabla c|^2}{y^3(z^2+x^2)^2})\} + \{(\Omega x(1-4c)$$

$$+RT[x\ln\frac{c}{1-c} + x + \frac{cx}{1-c}])(\frac{|\nabla c|^2}{zy(z^2+x^2)(y^2+x^2)}) + (\Omega\frac{c}{y}(1-2c)$$

$$+RT[\frac{c}{y}\ln\frac{c}{1-c}])(\frac{1}{y(z^2+x^2)} - \frac{2|\nabla c|^2}{y(z^2+x^2)^2(y^2+x^2)})\}] \tag{3.51}$$

47

and

$$
\begin{aligned}
\frac{\partial f_3}{\partial |\nabla c|} \;=\; & [\{(\Omega y(1-4c) + RT[y \ln \frac{c}{1-c} + y + \frac{cy}{1-c}])(\frac{|\nabla c|^2}{xz(y^2+x^2)(z^2+y^2)}) + (\Omega \frac{c}{z}(1-2c) \\
& + RT[\frac{c}{z} \ln \frac{c}{1-c}])(\frac{1}{z(z^2+x^2)} - \frac{2|\nabla c|^2}{z(z^2+x^2)^2(z^2+y^2)})\} + \{(\Omega x(1-4c) \\
& + RT[x \ln \frac{c}{1-c} + x + \frac{cx}{1-c}])(\frac{|\nabla c|^2}{zy(z^2+x^2)(y^2+x^2)}) + (\Omega \frac{c}{z}(1-2c) \\
& + RT[\frac{c}{z} \ln \frac{c}{1-c}])(\frac{1}{z(y^2+x^2)} - \frac{2|\nabla c|^2}{z(y^2+x^2)^2(z^2+z^2)})\} + \{(-\frac{2\Omega c^2}{z^2} \\
& + RT[\frac{c}{z^2} + \frac{c^2}{z^2(1-c)}])(\frac{|\nabla c|^2}{z^2(y^2+x^2)^2}) + (\Omega \frac{c}{z}(1-2c) \\
& + RT[\frac{c}{z} \ln \frac{c}{1-c}])(\frac{1}{z(y^2+x^2)} - \frac{|\nabla c|^2}{z^3(y^2+x^2)^2})\}]
\end{aligned}
\tag{3.52}
$$

Inserting eq:3.50, eq:3.51 and eq:3.52 in eq:3.46 to evaluate $\frac{\partial f_0^2}{\partial |\delta c|^2}$, through which 'k' can be determine by using eq:3.43. And then by eq:3.28 interfacial energy can be found by inserting the value of γ, k, β, T_c.

3.4   Free energy density for ZnO nanowires

For temperature less then conjugate temperature that is '$T < \frac{\Omega}{2R}$' there exist two minima, which corresponds distinct phases for Zn and O. For '$T = \frac{\Omega}{2R}$' both phases overcome the barrier and both are in dynamic equilibrium. As temperature approaches '$T > \frac{\Omega}{2R}$' the barrier is overcome by free energy density, and there is phase change.
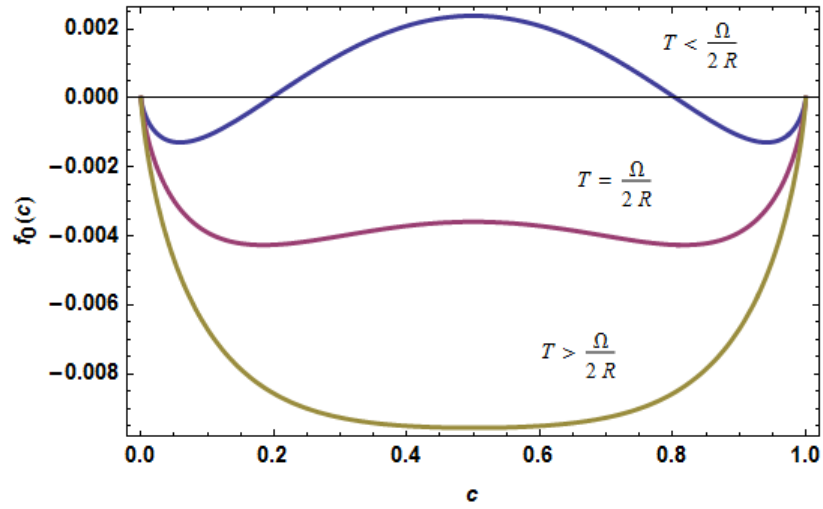
Figure 3.1: Free energy density as function of concentration

3.5 Interfacial Energy for ZnO nanowires

As temperature less then T_c molecule for Zn and O have not enough energy to overcome the interface and form new phase, as temperature become equal to T_c both phases attain energy but unable transform into another phase. As temperature increases above T_c interfacial energy overcome by constitutes and forming new phase.
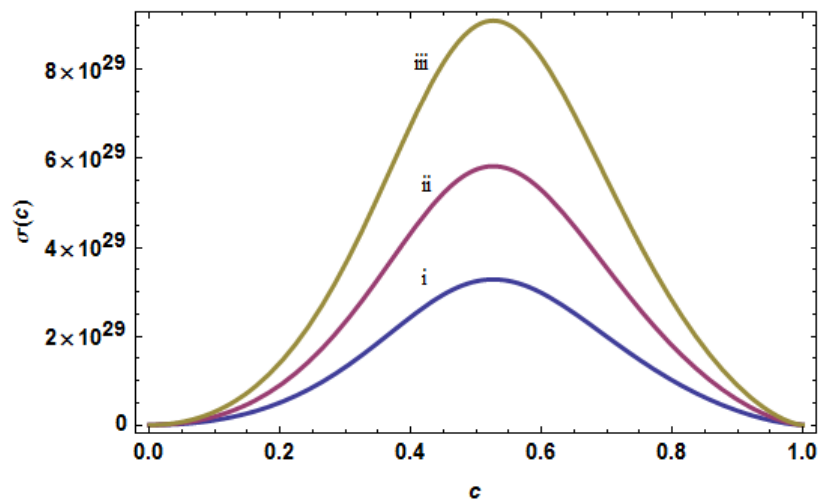
Figure 3.2: Interfacial energy as a function of concentration for 1-Dimensional structure for iii- $T < \frac{\Omega}{2R}$, ii- $T = \frac{\Omega}{2R}$, i- $T > \frac{\Omega}{2R}$.

3.6   Synthesis Process

Nano sized martials can be synthesized in a numerous technique like Hydrothermal, sol-gel, co-precipitation, vapor-liquid-solid (VLS) etc. Hydrothermal technique has advantages over the rest of technique for synthesizing 1-dimensional structure, because by using the suitable surfactant diameter cam be controlled, and doping can be made possible. Where as other technique like VLS technique have no control on diameter.

3.6.1   Hydrothermal Process

A synthesizing single crystal in aqueous media in an autoclave or crystallization technique in which precursors are dissolved in water and kept under elevated temperature and pressure in autoclave. Hydrothermal technique is a special case of solveothermal technique (chemical reaction taking place in a solvent under high temperature mostly above boiling temperature). Different structure can be synthesized in a closed system in an aqueous medium at temperature and pressure above then 100^0C and 1 atm. Hydrothermal method exploits that different properties of solvent such as dielectric constant, thermal conductivity viscosity etc. can be tuned by changing temperature and pressure. Key parameters for synthesizing any material in hydrothermal technique are temperature, pressure, duration and initial pH. This method shows the ability of water to dissolve substance at high temperature which are insoluble at lower temperature like some oxides, sulphides, silicates etc..

Hydrothermal technique have advantages over the other technique like Sol-gel, co-precipitation method etc. due to crystallization of those material made possible which are unstable at melting point, it also help for synthesising those material which require high vapor pressure. As for concern of crystalizing control growth can be made possible by changing thermal variable which remains until reaction has completed.

3.6.2 ZnO nanowires by Hydrothermal Process

2.97481g of Zinc Nitrate Hexahydrate $(Zn(NO_3)_2.6H_2O)$ dissolved in 10ml distilled water to obtain 1M solution. Now dissolving 1.921716g of Ammonium Carbonate $(NH_4)_2CO_3$) in 20ml distilled water to make 1 molar solution. Now slowly dropping 10ml of $(Zn(NO_3)_2.6H_2O)$ in 20ml of $(NH_4)_2CO_3$) and stirred at 800 rpm(revolution per minute) with help of hotplate. By using centrifugation process repeatedly at 1000 rpm to separate precipitate from residual reactant. This is done by using centrifuge machine. Obtained precipitate was dispersed in 70ml of 1% Polyethylene glycol (PEG) by sonicator for 20 minutes without heating. Obtained solution is added in Teflon cup and placed in Auto-calve and screw are tightly held such that to avoid pressure and temperature leakage. Finally Auto-calve is placed in Drying Oven for approximately 14 hours, obtained suspension was rinsed with water and ethanol with help of centrifugation. At the end the ZnO powder was obtained. Schematically this process is shown in figure 3.3.
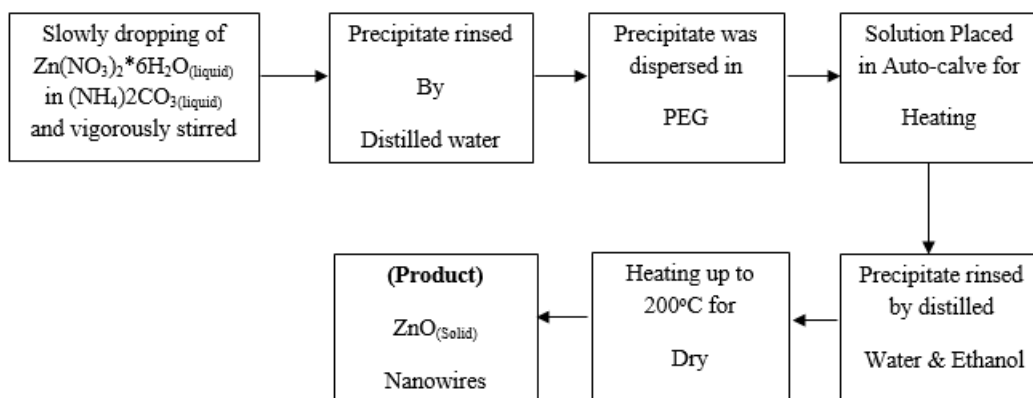
Figure 3.3: Schematic diagram for synthesis of ZnO nanowires

3.6.3 Carbon doped ZnO nanowires by Hydrothermal Process

For the synthesis of carbon doped ZnO nano-structures there need a improvisation in above preparation method. After rinsing obtained participate in 5 step with distilled water and ethanol we add 4% by weight activated carbon and crush with mortar and pestle for 5 minutes and left for heating at 700^oC for 4 hours. Schematically this process is shown in figure 3.4.
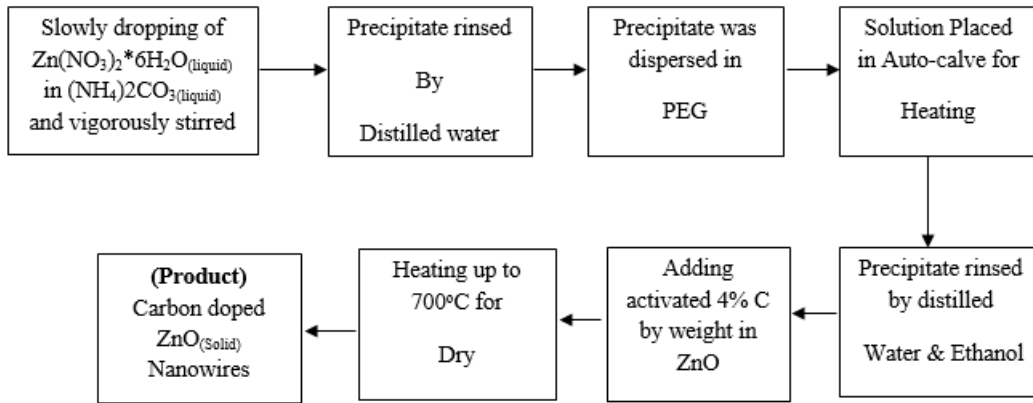
Figure 3.4: Synthesis process for Carbon doped ZnO nanowires.

Series of experiments had done with different percentages of PEG which are listed in table:3.1

Table 3.1: Synthesis menu for ZnO and C-ZnO

No.	$Zn(NO_3)_2.6H_2O$	$(NH_4)_2CO3$	PEG	Carbon
1	10 ml 2.97481g 1M	20 ml 1.921716g 1M	1%	4%
2	10 ml 2.97481g 1M	20 ml 1.921716g 1M	5%	4%
3	10 ml 2.67734g 1M	20 ml 1.921716g 1M	10%	4%
4	10 ml 2.67734g 1M	20 ml 1.921716g 1M	15%	4%
5	10 ml 2.67734g 1M	20 ml 1.921716g 1M	20%	4%

3.7 Characterization

3.7.1 Scanning Electron Microscopy (SEM)

SEM is used to obtained surface topography along with composition, water free sample are illuminated with coherent beam of electrons generated by tungsten filament. Backscattered, secondary and auger electron in company with x-ray are formed as shown in figure 3.5 which are detected with suitable detector and converted to images with raster scan pattern.
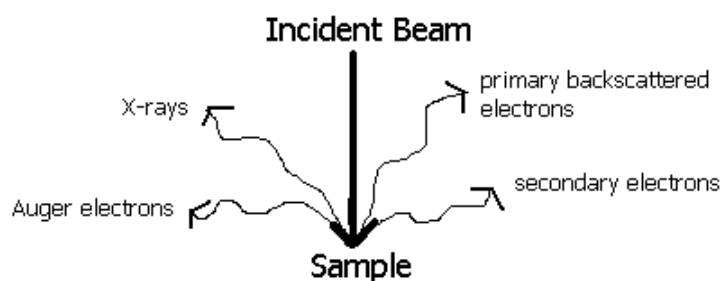
Figure 3.5: Working principle for SEM.

3.7.2 X-Ray Diffraction (XRD)

XRD is used to determine the crystal structure, lattice constants, lattice strain and planes. It works on the principle that when sample is impingement by coherent beam of X-rays constructive and destructive interference pattern is formed satisfying Bragg's Law ($n\lambda = 2d\sin\theta$), which relates the wavelength of incident and diffracted X-ray and diffraction angle. All possible orientations are obtained by scanning through 2θ, drawing percentage intensity for diffracted X-ray Vs 2θ gives the XRD pattern for specific material. Periodicity of crystal is defined by 3-D translation, rotation and reflection symmetry etc. These symmetry operations originates the crystallographic point group belonging to each of seven crystal system. The requirement for these symmetry operations for atomic coordinate say x,y and z same type of atoms and surrounding environment has to be there.

3.7.3 Energy dispersive X-ray (EDX)

EDX is used to determine the elemental composition and it is harmonious with SEM, X-rays generated by electron beam have characteristic energy which is related to specific element of specimen. X-ray detector convert the x-rays to voltage pulses by 'plus processor' hight of voltage pulse is related to energy of X-rays.

3.7.4 UV-Vis spectroscopy

Ultraviolet-visible spectroscopy is an absorption technique within incident beam of intensity of ultraviolet and visible region of electromagnetic spectrum. When light falls on material it excite the π electrons (non-bonding electrons) to highest level which falls on back emit an energy equals to energy deference between different energy bands. When the wavelength of incident radiation is resonant with energy difference between two antibonding states, it absorbed by the material, which compared with reference wavelength to find the specific wavelength at which it is absorbed by material, schematic diagram is shown in figure3.7. Corresponding energy is band gap energy of material $E_g = \frac{hc}{\lambda}$.

3.7.5 Fourier transform infrared spectroscopy (FTIR)

FTIR spectroscopy is used to study the bonding structure of martial and to identify different chemical group presents in a sample. FTIR spectroscopy uses infrared rays to draw vibrational and associated rotational spectra.

In solid material atoms vibrates around their mean position in a crystal lattice which is also known as phonon (lattice vibrations). These lattice vibrations depends on interatomic force, bond energy and masses, and these are intrinsics properties of material so different materials have different lattice vibrations. Quantum mechanical picture shows that even at zero temperature these vibrations
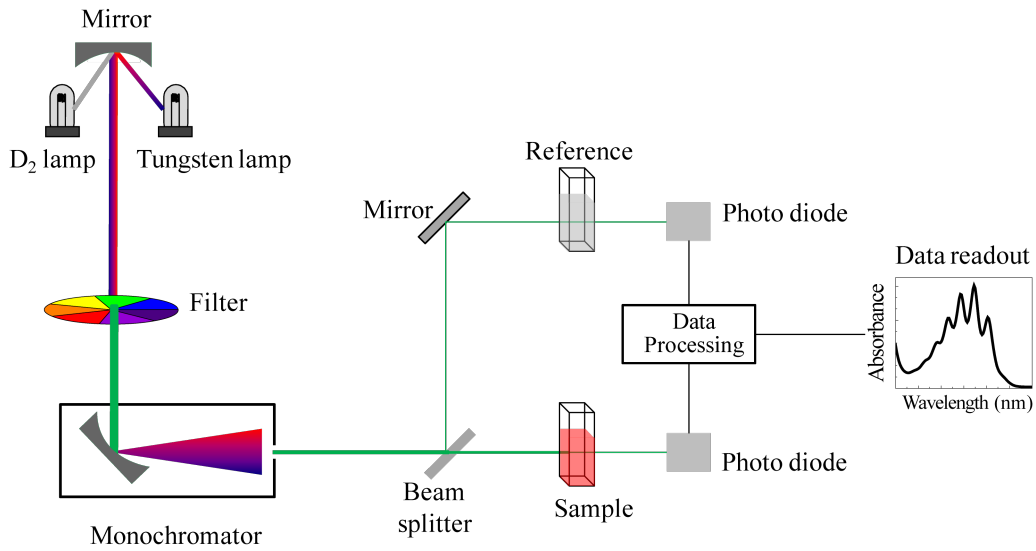
Figure 3.6: Schematic diagram for FTIR analysis.

exist.

$$E_n = (n+1)\hbar\omega \qquad n = 0, 1, 2, 3....$$ (3.53)

where 'n' is mode number corresponds to different vibrational frequency ω , for n=0, $E_0 = \hbar\omega$ is ground state energy. Different lattice sites vibrating with different frequency, when infrared light is passed if it resonant with lattice vibrational frequency it absorbs and if there is mismatch then incident infrared light transmit through it. Absorbed intensity is compared with reference one, which gave the absorbed spectra. systematical diagram is presented in figure 3.7. Through this technique several analysis such as surface bonding, identification of unknown material and quality of sample can be determined.

3.7.6 LCR

Dielectric material store energy and neutralize the charges at plates (electrodes). When AC voltage is applied to electrode equivalent circuit can be drawn shown in figure 3.8. Incident current is sum
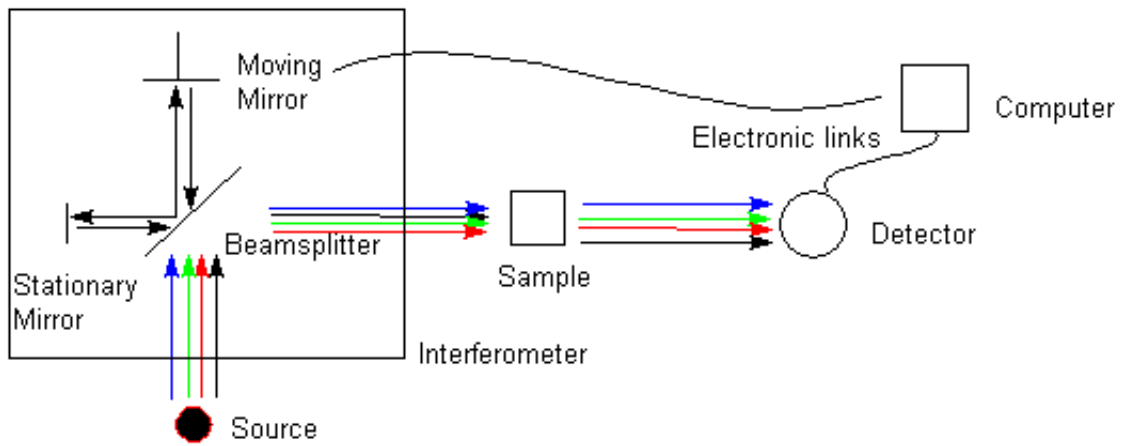
Figure 3.7: Schematic diagram for FTIR analysis.

of conduction current (l_c) and loss current (l_s) due to dielectric material present;

$$I = I_c + I_l \tag{3.54}$$

The losses in the material can be represented as a conductance (G) in parallel with a capacitor (C).

$$I = V(j\omega C_0 \varepsilon' + G) \tag{3.55}$$

whereas conductance 'G' is defined as $G = \omega C_0 \varepsilon"$, inserting in above equation we get;

$$I = V(j\omega C_0)(\varepsilon' - j\varepsilon") = V(j\omega C_0)\varepsilon \tag{3.56}$$
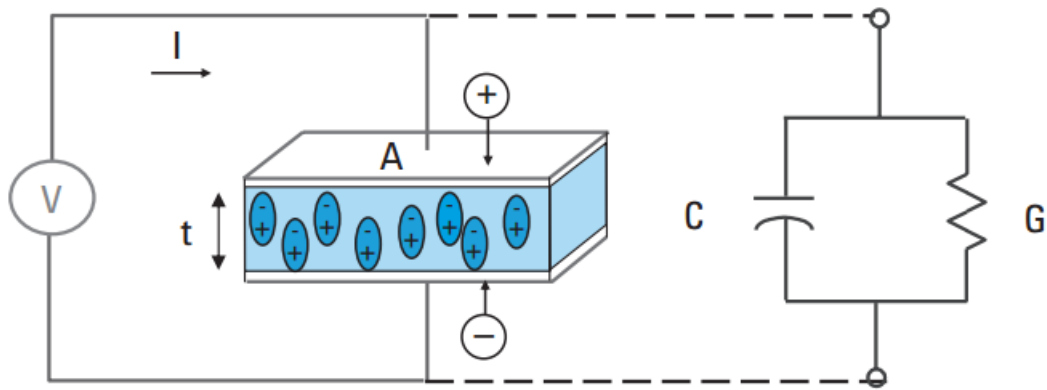
Figure 3.8: Parallel plate capacitor and equivalent LR circuit for dielectric measurement.

3.8 Summary

Nucleation of single crystal can be thought of total free energy available for a system. This energy must be enough to overcome interface energy between two different phases, where as interfacial energy is a function of gradient concentration and temperature. Due to spatial variation in concentration interfacial energy has different statistics in 1-D, 2-D and 3-D system. With the help of interfacial energy one can determine the nucleation rate.

When two phases are in contact its better to include mixed internal energy and entropy rather then intrinsic one, mixed internal energy and entropy helps to calculate free energy density through conjugate temperature or critical temperature can be formulated which helps to pre-determine the nucleation of different phases at specific temperature.

Interfacial energy for 1-D ZnO shows that synthesis is possible even not at elevated temperature, using different quantity of surfactant and at different temperature slow nucleation made possible through hydrothermal synthesis, as slow nucleation form elegant structure. synthesis of C-doped ZnO is made possible at specific value of surfactant due to control growth.

Chapter 4

Results and Discussions

4.1 XRD Analysis

XRD pattern for ZnO and Carbon-doped ZnO in figure 4.1 obtained by irradiating with K_α of Cu source of wavelength 1.54 . The obtained pattern is analyzed with MDI Jade 6.5 using PDF (Powder Diffraction File) card number **36-1451**. ZnO is Wurtzite structure $a \times b \times c$ $\langle 90^0 \times 90^0 \times 120^0 \rangle$ where a, b and c are lattice constant and values in Å. Calculating the average lattice constant for above obtained pattern it comes out to be $3.2495 \times 3.2495 \times 5.2076$ $\langle 90^0 \times 90^0 \times 120^0 \rangle$ deviating $0.009\% \times 0.009\% \times 0.019\%$ whith actual values for lattice parameter $3.2498 \times 3.2498 \times 5.2066$.

When Carbon is added in ZnO the lattice parameter comes out to be $3.2414 \times 3.2414 \times 5.3969$ $\langle 90^0 \times 90^0 \times 120^0 \rangle$ deviating $0.25\% \times 0.25\% \times 3.65\%$ with actual lattice parameter of ZnO. Crystalize size (cz)is calculated by using Scherrer's formula:

$$D_p = \frac{k\lambda}{\beta cos\theta} \tag{4.1}$$

where D_p is means radius of highest intensity peak, k is shape factor usually taken 0.9, β is Full Width Half Maximum (FWHM) and taken in radians and θ is Bragg's angle. Providing above information cz has been calculated for ZnO and C-ZnO at different percentages of PEG as shown in table 4.1. We observed that elevation in cz at $1\% \rightarrow 15\%$ but at 20% it demotion is observed.
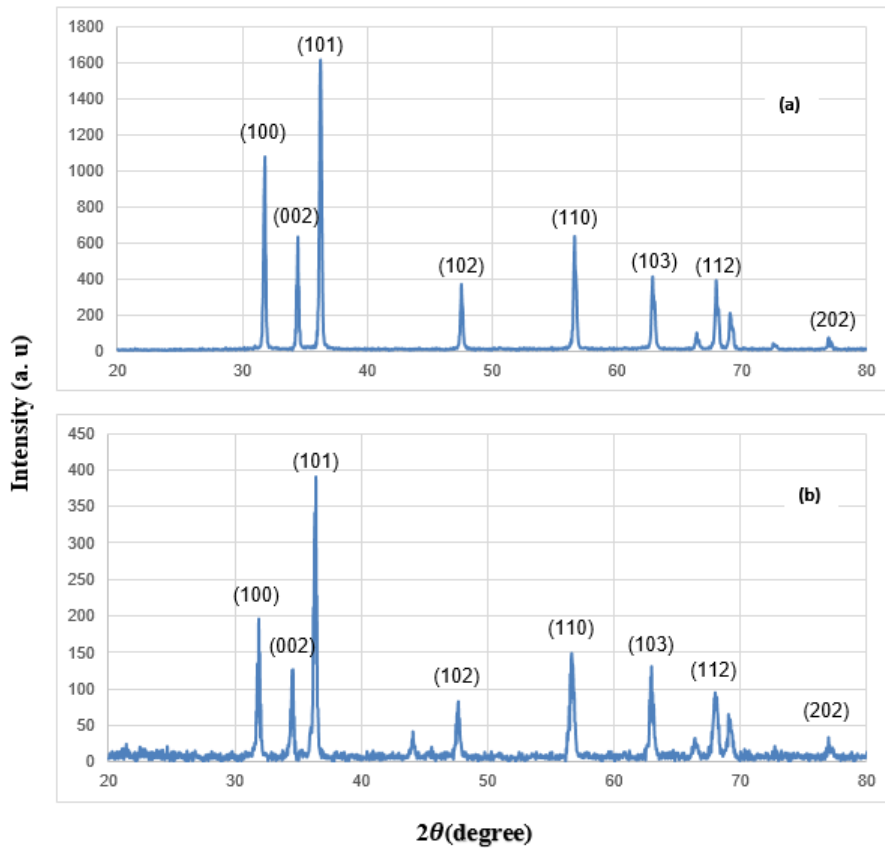
Figure 4.1: XRD pattern for ZnO (a) without carbon and (b) doped with 4 weight percentage of carbon.

Another observation is that cz for C-doped ZnO is greater then ZnO and decreases at 20% with greater percentage.

Lattice strain is defined by dislocation in lattice parameter due crystal environment and lattice hardening or cold working is defined as dislocation of lattice after plastic deformation. Lattice strain from XRD pattern can think of broadening of gaussian obtained, sharper the peak decrement in gaussian broadening and crystal is brittle so little stress is required to deform. Lattice strain is calculated for the XRD pattern obtained for ZnO and C-ZnO figure 4.1 for different percentage of PEG is shown in table4.1, another result can considered that there is decrement in lattice strain as there is increment is observed in crystalize size.

Table 4.1: Crystalize size and Lattice strain for ZnO and C-doped ZnO at different percentages of PEG.

PEG	Crystalize Size(nm)		Lattice Strain	
	ZnO	C-ZnO	ZnO	C-ZnO
1%	41.4	44.1	0.0028	0.0026
5%	43.89	46.46	0.0027	0.0025
10%	46.96	48.28	0.0025	0.0024
15%	48.26	46.7	0.0024	0.0025
20%	44.56	36.39	0.0026	0.0032

4.2 Fourier transform infrared spectroscopy (FTIR)

FTIR spectroscopy is used to study the bonding structure of martial and to identify different chemical group presents in a ZnO. Basic purpose of doing this to find an appropriate lattice site suitable for dopant (carbon), because carbon is nonmetallic it will react with Oxygen present in ZnO and destroy the structure. So its necessary to find exact bonding structure.

Figure 4.2 shows the FTIR spectra taken at room temperature, peak arises at 520 cm^{-1} corresponds to wurtzite hexagonal phase of ZnO. Peak arises at 1394 cm^{-1} and 1553 cm^{-1} corresponds to carboxylate group (COO^{-1}) due to Ammonium Carbonate present in precursor. Peak at 2933 cm^{-1} and 3479 cm^{-1} due to C-H (acetate) and O-H group.

So there are two possible lattice sites available for carbon doping, one is Zn and the other is Oxygen site. One should be careful such that doping should be such that it will change the physical property retaining the crystal structure same. This could be done by reducing the surface available for interaction with dopant, in other words reducing the surface energy such that carbon interacts to only few surface available for interaction. In our experimentation we uses PEG as surfactant, main function of surfactant is to reduce surface energy by making micelle formation of himself at the surface. So FTIR spectroscopy helps us to find the possible lattice site available for bonding with dopant material (Carbon).
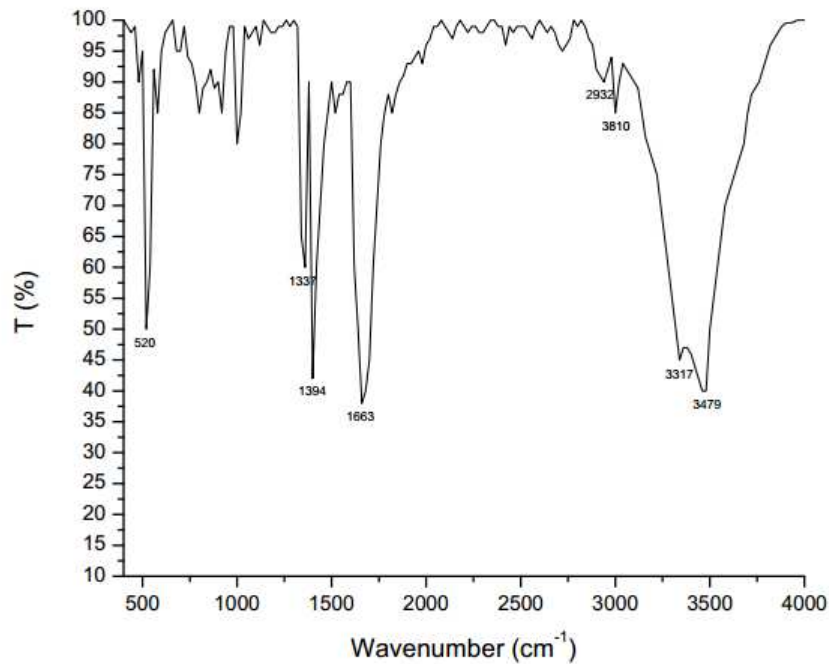
Figure 4.2: FTIR reflection spectra of ZnO nanowires.

4.3   Scanning Electron Microscopy (SEM)

In figure 4.3 SEM images are shown at different magnification power X2,500 and X15,00 for ZnO when the surfactant PEG is 10% is used. SEM analysis confirms that nanowires are obtained with avg. diameter $44.6nm$ and avg. length $0.64\mu m$. where as when 4% by weight activated
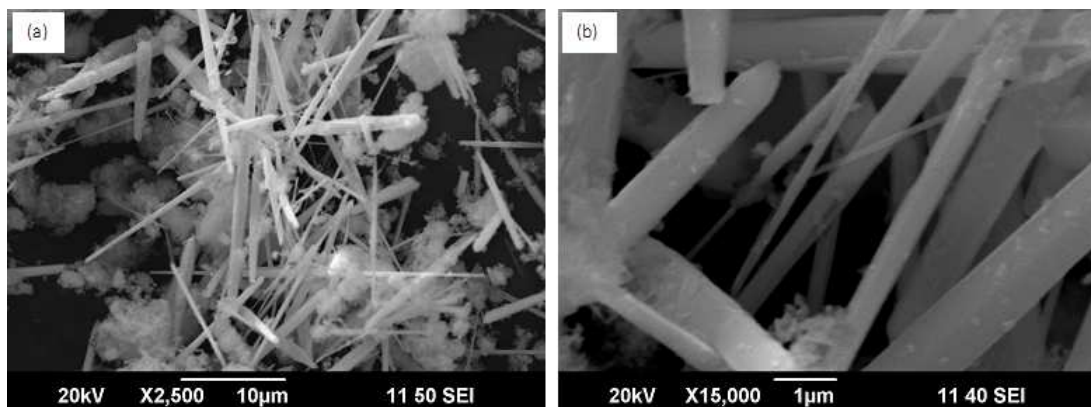
Figure 4.3: SEM images of ZnO nanowires by using 10% PEG

carbon is added there is increment in diameter and length of nanowires. In figure 4.4 shows the

1-dimensional structure for C-ZnO with avg. diameter $69.28 nm$ and avg. length $16.7 \mu m$.
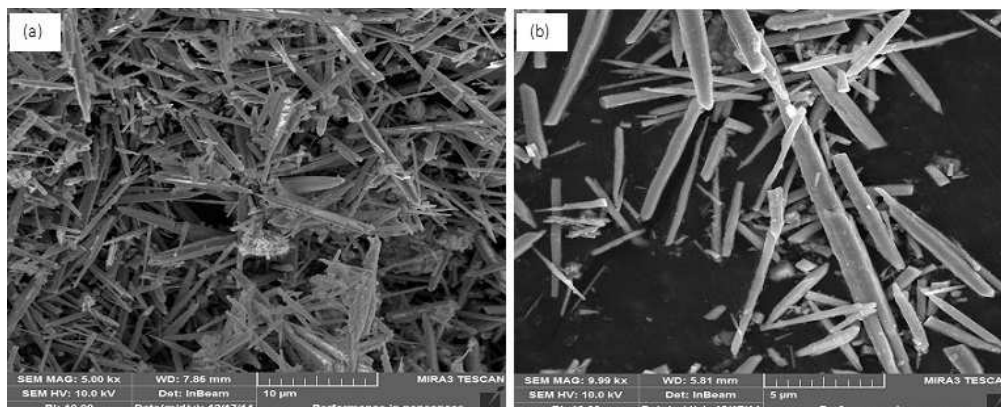
Figure 4.4: SEM images of Carbon doped ZnO nanowires by using 10% PEG

Results obtained by using different percentages of surfactant $1\%, 5\%, 10\%, 15\%, 20\%$ are shown in table:4.2. Following are anomalies observed at $1\%, 15\%, 20\%$ especially for C-ZnO:

1. There is increment in diameter for ZnO.

2. At $1\%, 15\%, 20\%$ there is nothing found in SEM for C-ZnO shown in figure 4.5.

3. There is increment in length, but at 20% SEM analysis unable to find appropriate length.
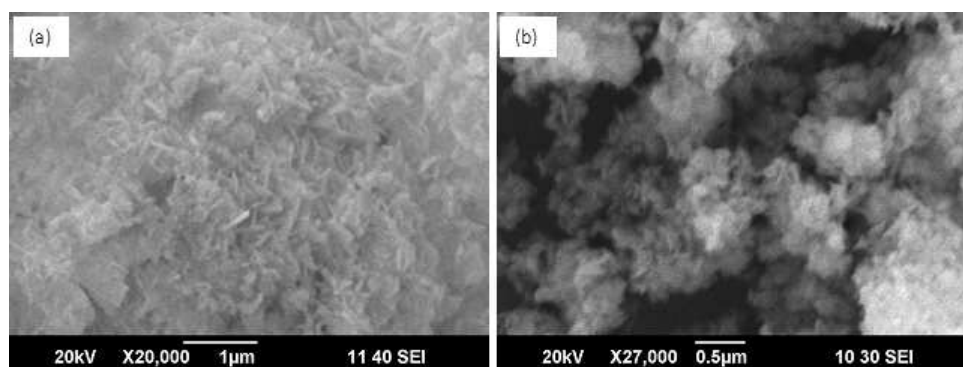
Figure 4.5: SEM images for Carbon doped ZnO at (a) 1% PEG (b) 15% PEG

Table 4.2: Avg. diameter and length for different percentages of PEG for ZnO and C doped ZnO

PEG	Avg. Diameter (nm)		Avg. Length (μ m)	
	ZnO	C-ZnO	ZnO	C-ZnO
1%	63.91	Nil	25.99	Nil
5%	50.44	98.6	14.63	32.48
10%	54.29	98.97	0.64	16.67
15%	117.7	141.54	324.6	18.23

4.3.1 Why Carbon doped at specific percentage of PEG?

Electronic configuration of Zn atom is $[Ar]3d^{10}4s^2$ and for oxygen atoms $1s^22s^22p^4$, +2 oxidation state of Zn atoms forms sp^3 covalent bonding with four nearest neighbors of oxygen atoms. Due to having ionicity upto greater extent ZnO have substantial ionic character. Electronic configuration for Carbon atom is $[He]2s^22p^2$, it will disturb the sp^3 hybridization when it is doped. There are two lattice sites where carbon can reside first at Zn site which is hardly to occur because Zn atom is screened by four oxygen atoms other reason is that it is 5 times less then the atomic mass of Zn. In others words carbon atom has not enough momentum to replace Zn atoms. Second lattice site is oxygen site, where it can reside due to almost same atomic size. Substitution of C at oxygen lattice site also responsible for room temperature ferromagnetism (RTF). A strong coupling between carbon 2p and Zn 4s,3d, due to exchange interaction spin spilt state are formed. There is p-p exchange interaction in localized C2p and valance band electrons, these interaction carries magnetism along with due to large contribution by magnetic moments. And there is also small contribution by neighbouring Zn atoms and second nearest O atoms. This is already reported that C-ZnO has bond energy 323.23kj/mol for thin film at 800^0C. While we focusing on nanowires because by changing the diameter we can change band gap energy which is related to binding energy of constitute. For doping principle dopant material can alter the chemical and physical properties retaining the crystal structure same. Surface energy for hexagonal structure can be calculated from bond energy with help of relation as below:

$$\sigma_{\alpha\beta} = \frac{\sqrt{3}\varepsilon_{avg.}}{N_a a^2} \tag{4.2}$$

Surfactant adsorb at the surface and passivate the surface due to saturation in dangling bond at

the surface, In result lower the surface energy. And diffusion rate is to be determined by diffusion coefficient of the surfactant. Interface is created between surface atoms and surfactant atoms which limited the further diffusion. Which in result decrease the surface energy, the extent of decrement can be quantified by taking the surface energy as function concentration of surfactant added. For an ease surfactant to be considered as β phase and host material as an α phase. $c = \frac{N_\beta}{N_\alpha + N_\beta} = \frac{N_\beta}{N_a}$ is the fractional concentration of β phase and $1 - c = \frac{N_\alpha}{N_a}$ is the fractional concentration of α phase, fractional concentration are taken to avoid nonlinearity in a system. [38]

Addition of surfactant reduces the surface energy of host material by doing the work which can quantified as $W = \sigma_{\alpha\beta}\Delta a$. $\sigma_{\alpha\beta}$ is surface energy between respective phases and 'a' is the surface area of β phase molecule which changes with concentration of β phase. And defined as $a = N_\beta 4\pi r_h^2 = c N_a 4\pi r_h^2$, here an approximation of spherical symmetrical distribution of β phase molecules is applied. Where r_h is the stokes radius or hydrodynamic radius of molecule, which is taken because mostly surfactant molecules are organic compounds and exist in the forms of micelle or colloidal particle.

So for doping purposes surface energy can be tuned to such value where dopant can make bond with host material. For this As surfactant is added it changes the internal energy ε_0 (intrinsic) to ε_{mix} (extrinsic) and similarly entropy of system s_0 (intrinsic) to s_{mix} (extrinsic). From first of thermodynamics:

$$
\begin{aligned}
\Delta E &= \Delta Q - W \\
\varepsilon_{mix} - \varepsilon_0 &= T(s_{mix} - s_0) - \sigma_{\alpha\beta}\Delta a
\end{aligned}
\tag{4.3}
$$

After rearranging;

$$
\begin{aligned}
\sigma_{\alpha\beta} &= \frac{\varepsilon_0 - Ts_0 - (\varepsilon_{mix} - Ts_{mix})}{\Delta a} \tag{4.4} \\
\sigma_{\alpha\beta} &= \frac{f_0 - f_{mix}}{\Delta a} \tag{4.5}
\end{aligned}
$$

'f_{mix}' and 'f_0' are the free energy density or molar Helmholtz energy of mixed and intrinsic

solution. Further we can write as;

$$\sigma_{\alpha\beta} = \left(\frac{\partial f_{mix}}{\partial a}\right)_{NVT} \tag{4.6}$$

whereas;

$$f_{mix} = \varepsilon_{mix} - T s_{mix} \tag{4.7}$$

ε_{mix} is to be defined in term of sum of pairwise interatomic potential or enthalpy of formation $\varepsilon_{\alpha\alpha}, \varepsilon_{\alpha\beta}$ and $\varepsilon_{\beta\beta}$ between the molecules of α and β phases as;

$$\varepsilon_{mix} = P_{\alpha\beta}[\varepsilon_{\alpha\beta} - \frac{1}{2}(\varepsilon_{\alpha\alpha} + \varepsilon_{\beta\beta})] \tag{4.8}$$

$P_{\alpha\beta}$ are the number of bonds in a solution between respective phase which can be defined as;

$$P_{\alpha\beta} = z N_\alpha N_\beta = z N_a c (1 - c) \tag{4.9}$$

'z' is the nearest neighbours in the resultant phase ($\alpha\beta$).

s_{mix} is the mixed entropy which is to be defined by Boltzman relation $s_{mix} = k \ln \frac{W_{mix}}{W^0}$, W^0 and W_{mix} are number of ways in which the N_α and N_β can be arranged before and after mixing. Constraint $W^0 = 1$ for indistinguishable state is applied because particle are distributed classically. And $W_{mix} = \frac{N_a!}{N_\alpha! N_\beta!} = \frac{(N_\alpha + N_\beta)!}{N_\alpha! N_\beta!}$, so;

$$\triangle S_{mix} = k \ln \frac{N_a!}{N_0! N_s!} \tag{4.10}$$

Applying Stirling formula $\ln N! \approx N \ln N - N$ to above eq. we get:

$$\triangle S_{mix} = -R[(1 - c)\ln(1 - c) + c \ln c] \tag{4.11}$$

whereas $R = k N_a$. Inserting eq:4.8 and 4.11 in eq:4.8 we get;

$$f_{mix} = z N_a c (1 - c)[\varepsilon_{\alpha\beta} - \frac{1}{2}(\varepsilon_{\alpha\alpha} + \varepsilon_{\beta\beta})] + T R[(1 - c)\ln(1 - c) + c \ln c] \tag{4.12}$$

65

Now solving eq:4.6

$$\frac{\partial f_{mix}}{\partial a} = \frac{\partial f_{mix}}{\partial c}\frac{\partial c}{\partial a} \tag{4.13}$$

$$\frac{\partial f_{mix}}{\partial c} = zN_a(1-2c)\left[\varepsilon_{\alpha\beta} - \frac{1}{2}(\varepsilon_{\alpha\alpha} + \varepsilon_{\beta\beta})\right] + TR\left[\ln\frac{c}{1-c}\right] \tag{4.14}$$

$$\frac{\partial c}{\partial a} = \frac{1}{N_a 4\pi r_h^2} \tag{4.15}$$

Inserting eq:4.14 and 4.15 in eq:4.13

$$\sigma_{\alpha\beta} = \frac{\partial f_{mix}}{\partial a} = \frac{z}{4\pi r_h^2}(1-2c)\left[\varepsilon_{\alpha\beta} - \frac{1}{2}(\varepsilon_{\alpha\alpha} + \varepsilon_{\beta\beta})\right] + \frac{TR}{N_a 4\pi r_h^2}\left[\ln\frac{c}{1-c}\right] \tag{4.16}$$

Above equation is the surface energy density as function of concentration of β phase. Behavior of graph can be different because interatomic potential or bond energies for different constitute may be different.

4.3.2 Modulated surface energy of ZnO (α phase) with assistance of surfactant PEG (β phase):

Polyethylene Glycol (PEG) $H-(O-CH_2-CH_2)_n-OH$ soluble in water, so when it is diluted $(O-CH_2-CH_2)_n$ chain of ethylene oxide left, Enthalpy of formation for ethylene oxide is 354.38 kj/mole. And it forms micelles, stokes radius 'r_h' for PEG in water solvent is $7.6 \times 10^{-10}m$. As we are going to synthesize the 1-dimensional structure so stokes radius stretches out in a such a way to cover more of the space available. Enthalpy of formation between $\alpha\beta$ phase is taken zero, while for Zn-O ($\alpha\alpha$ phase) it is 250 kj/mol and for PEG ($\beta\beta$ phase) is 354kj/mol. ZnO has surface energy 11.53 j/m² and corresponding bond energy is 250 kj/mol. We lower the surface energy in such a way that carbon can make bond with ZnO which requires less formation energy. When concentration of PEG is in between 5% to 10% the surface energy modulates between 10.385j/m²
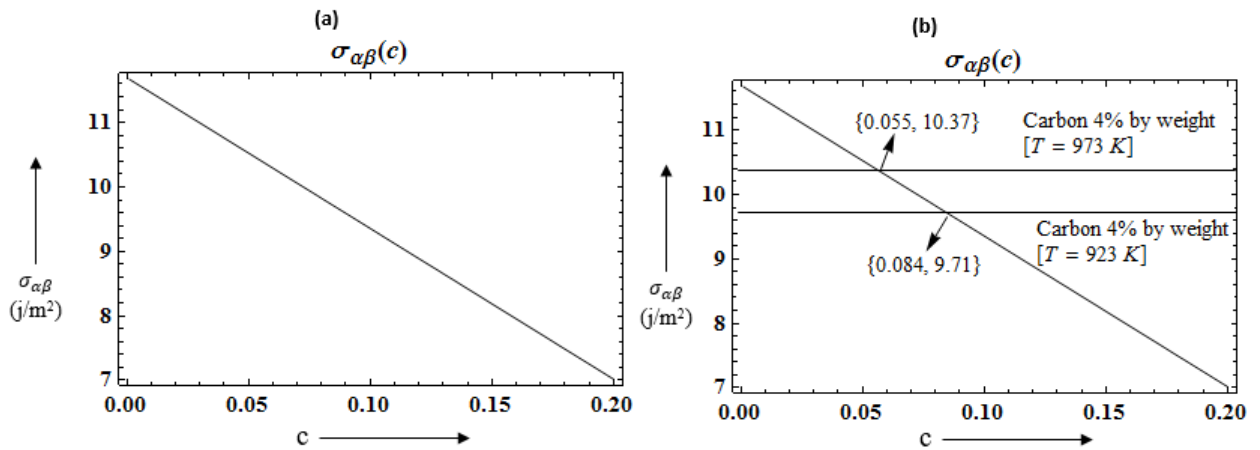
Figure 4.6: Surface energy as function of PEG concentration

to 9.785j/m^2 as shown in figure 4.6. So carbon with concentration 4% by weight can be doped at post growth temperature range temperature range 650 to 700^0C.

4.4 Energy dispersive X-ray (EDX)

4.4.1 EDX of ZnO

Figure 4.7 shows the EDX analysis for ZnO. Oxygen peak observed at 0.525 keV while Zinc peaks are observed 1.01, 8.63 and 9.58 keV, this distribution corresponds to pure ZnO. Gaussian peaks for Zn and O at specific energies while 10% of PEG as surfactant has been used.
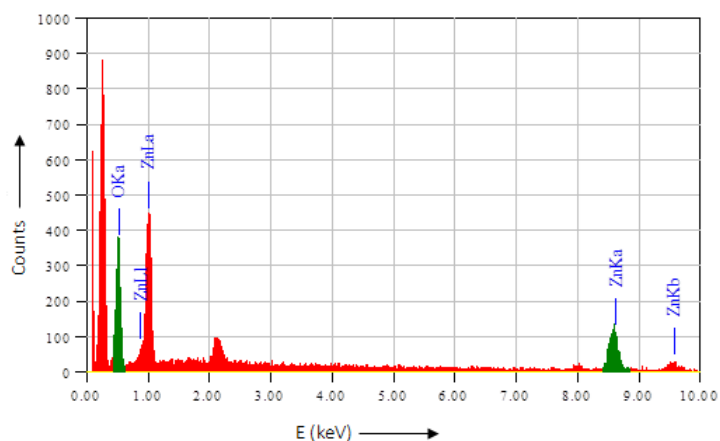
Figure 4.7: EDX for ZnO at 10% of PEG

4.4.2 EDX of C-ZnO

Figure 4.8 shows the EDX analysis for C-ZnO. 4% by weight doping of carbon in ZnO gives an extra peak at 0.277 keV while other peaks observed at same peaks as above but with different intensity. This difference in intensity is due to free electrons provided by carbon make more easier transition for electrons.

Figure 4.8: EDX for C-ZnO at 10% of PEG

All the above results can be confined in below table where we can can see that as carbon is doped it replace oxygen as well as Zn.

Table 4.3: EDX for ZnO and C-ZnO

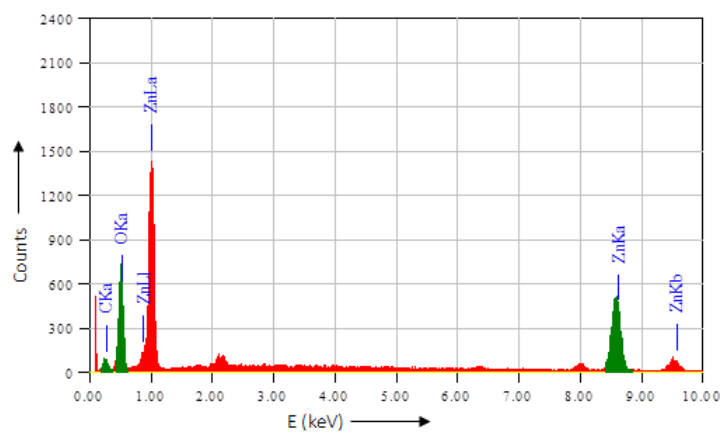| Element	E(keV)	%Mass	%Error	%Atom	K
O K	0.525	50.09	1.82	80.39	57.1171
Zn K*	1.01,8.63,9.58	49.91	12.16	19.61	42.8829
Total		100		100	
Carbon doped ZnO					
C K	0.277	37.34	0.3	53.67	17.9963
O K	0.525	36.53	0.78	39.42	39.9783
Zn K	1.01,8.63,9.58	26.14	2.68	6.9	42.0255
Total		100		100	

4.5 UV-Vis spectra

Figure 4.9 shows the absorption spectra for ZnO and C-Zno nanowires. Absorption peak for ZnO nanowires observed at 364nm, and for C-ZnO at 367nm. Corresponding bandgap is E_g= 3.4062 eV for ZnO and E_g= 3.3783 eV for C-ZnO. This change in band gap due to free electron preserved by Zn atom as carbon replaces oxygen atom. Second peak at the wavelength of 523nm for C-ZnO is due to lateral surface defects. As carbon is doped it enforce the crystal structure of ZnO to reorient, which is the cause of defects in crystal. Two types of defects can be found in crystal lattice, that are the Frenkel defect and Schottky defect. The Frenkel Defect is a defect in the lattice crystal where an atom or ion occupies a normally vacant site other than its own. Second one is the Schottky defect which is the defect forms when oppositely charged ions leave their lattice sites, creating vacancies.
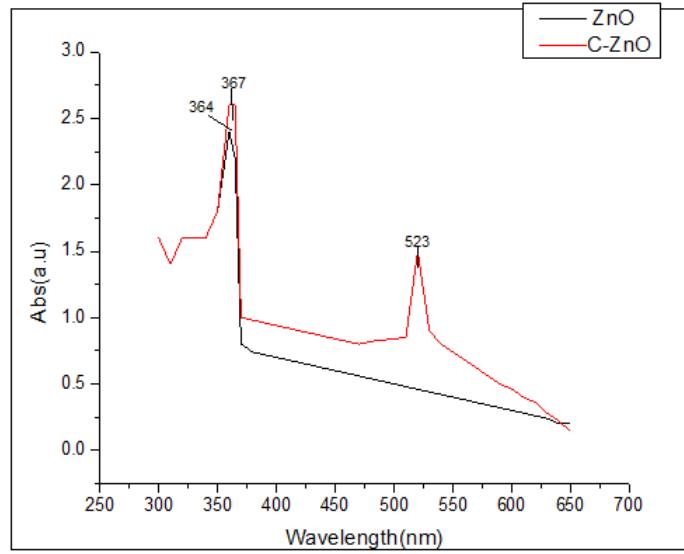
Figure 4.9: Absorption spectra for ZnO and C-ZnO.

Electronic configuration of Zn atom is $[Ar]3d^{10}4s^2$ and for oxygen atoms $1s^2 2s^2 2p^4$, $+2$ oxidation state of Zn atoms forms sp^3 covalent bonding with four nearest neighbors of oxygen atoms. Due to having ionicity upto greater extent ZnO have substantial ionic character. Electronic configuration for Carbon atom is $[He]2s^2 2p^2$, it will disturb the sp^3 hybridization when it is doped. So second arises due to Schottky defect present in crystal structure.

4.6 Dielectric Properties of ZnO and C-ZnO

Dielectric constant of ZnO and C-ZnO is determined through LCR (Inductance, Capacitance, Resistance) meter. When material is subjected to AC electric field, dipole existed in material align themselves in direction of applied field or in other words dipole gets polarized. So variation in dielectric constant with respect AC frequency is due to change in polarization.

4.6.1 Dielectric constant of ZnO

Figure 4.10 shows the variation of dielectric constant for ZnO as a function of frequency of applied AC electric field. At lower frequency weak polarization such as ionic and dipolar polarization con-

tributes to dielectric constant. At higher frequency contribution towards dielectric constant from weaker polarization is no more effective, because field switches so fast such that the dipoles can not reorient in direction of applied field. At higher frequency electrotonic and atomic polarization dominates, as these polarizations are long lived because they switches the polarization so fast according to frequency of applied field. So constant region of dielectric constant is due to electronic and atomic polarizations. And at the end dielectric drops to zero because frequency is too high enough which destroy the electronic polarization and this frequency is known as cutoff frequency after this frequency material is no more dielectric.
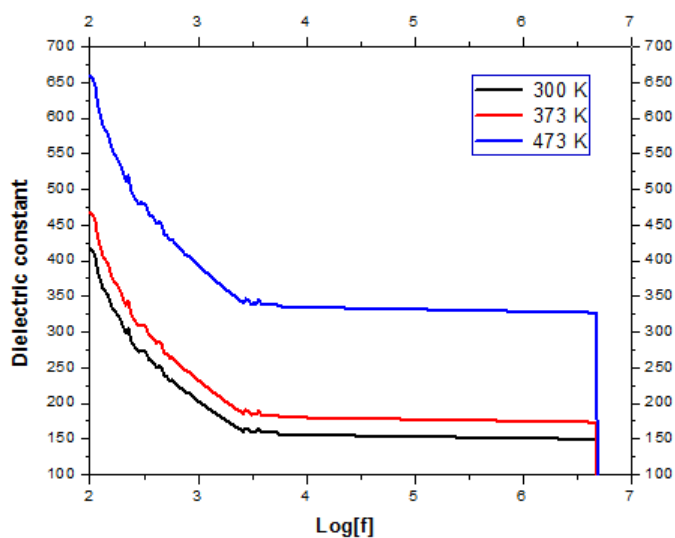
Figure 4.10: Dielectric constant of ZnO at temperature 300K, 373K and 473K.

4.6.2 Dielectric constant of C-ZnO

Figure 4.11 shows the variation of dielectric constant of C-ZnO as a function of frequency of applied AC electric field. In lower regime weak polarization take places in dielectric constant, but at higher frequency atomic and electronic takes places. Slight rise in dielectric constant at higher frequency is due electronic polarization. As when carbon replaces oxygen it presents some ionic character which are not prominent at low frequencies because dopant (carbon) is of very few percentage is used to avoid lattice deformation. As the frequency increases these polarization also taking part in dielectric constant. Rise of dielectric constant for C-ZnO is due to extra polarizablity

71

presented by carbon atom.
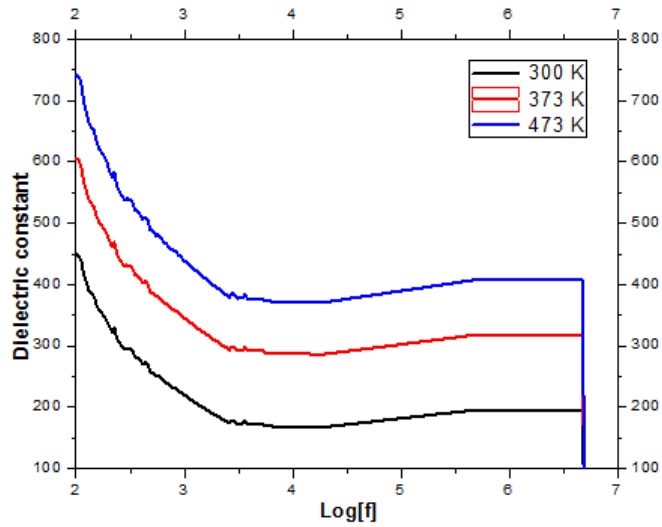
Figure 4.11: Dielectric constant of C-ZnO at temperature 300K, 373K and 473K.

4.6.3 Temperature dependence of dielectric constant of ZnO and C-ZnO

In a ferroelectric medium, the dipoles are already aligned and, unless the outer field is very strong, thus do not contribute to the orientational polarizability. High temperature disturbs the ferroelectric alignment and produces molecules that are free to reorient in an external field, and these contribute to the dielectric constant. So from results shown in figure 4.10 ZnO and for C-ZnO in figure 4.11, it confirms that these are ferroelectric materials. Because Dielectric in both cases increases with temperature.

4.6.4 Tangent loss of ZnO

Complex dielectric is defined as:

$$\epsilon = \epsilon' - \iota\epsilon'' \tag{4.17}$$

72

Where ϵ' is the real part of dielectric constant and ϵ'' is the complex part of dielectric constant which is also known as dielectric loss. Its better to defined tangent loss for material which is defined as the ratio (or angle in a complex plane) of the lossy reaction to the electric field E in the curl equation to the lossless reaction:

$$\tan \delta = \frac{\epsilon''}{\epsilon'} \qquad (4.18)$$

Figure 4.12 shows the variation of tangent loss for ZnO as a function of frequency of applied AC electric field. It shows that as frequency increases tangent loss also decreases. A little rise is observed in lower frequency regime because atoms are rearranging and behaving as free radical for short time or in other words bonds re stretches and try to realigned in new direction so they conduct the applied field rather than storing in form of energy. As the temperature increases more free radical are formed which increases the complex part of dielectric constant, hence tangent loss increases.
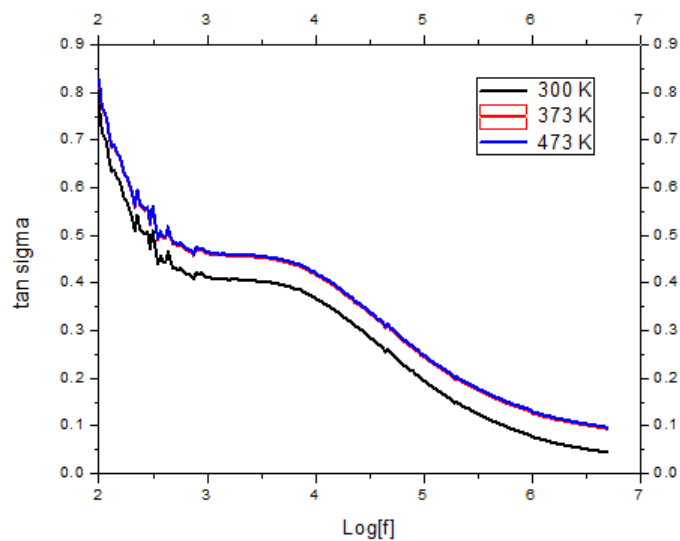

Figure 4.12: Tangent loss for ZnO at temperature 300K, 373K and 473K.

4.6.5 Tangent loss of C-ZnO

Figure 4.13 shows the variation of tangent loss for C-ZnO as a function of frequency of applied AC electric field. Same trends is found as for ZnO and there is no significant difference is found with respect to temperature in tangent loss because dipole moment presented by C-ZnO are strong enough such that the little thermal agitation didn't disturb the dipolar polarization. This fact can also be stated as for higher temperature because most of the dipole are get saturated so this effect loss.
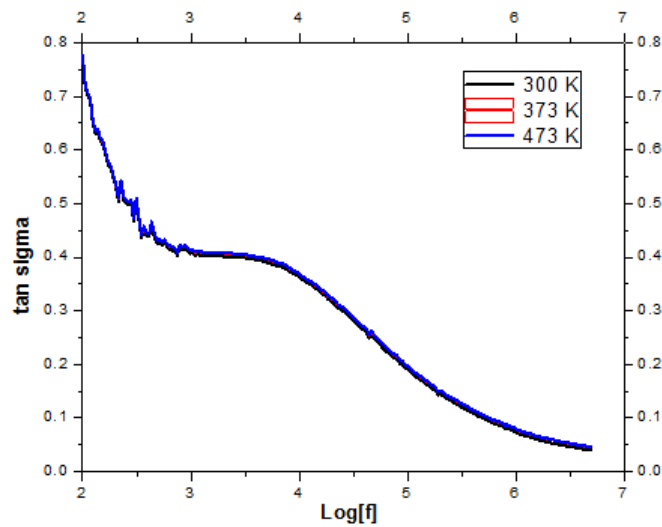
Figure 4.13: Tangent loss for C-ZnO at temperature 300K, 373K and 473K.

4.6.6 AC conductivity of ZnO and C-ZnO

Figure 4.14 shows the variation of AC conductivity as a function of frequency of applied AC electric field. AC electrical conductivity of material can be calculated by using following relation:

$$\sigma_{ac} = \omega C \tan \delta \times \frac{d}{A} = \epsilon'' \omega \epsilon_0 \tag{4.19}$$

Where $\omega = 2\pi f$ is angular frequency of applied AC field, 'C' is the capacitance of the pallets (material should used in term of defined shape, which helps us to find the thickness and area of the shape which is useful for further calculation), 'd' is the thickness of pallet and 'A' is the area

of the pallet. AC conductivity response for ZnO and C-doped ZnO nanowires are shown in figure 4.14. As from Dielectric measurement it is clear that C-ZnO has higher dielectric so conductive response is lesser.

As the frequency of current is too high all the dipole formed in material are broken and free radicals are formed which is now conduct like conductor and AC conductivity shoots out.
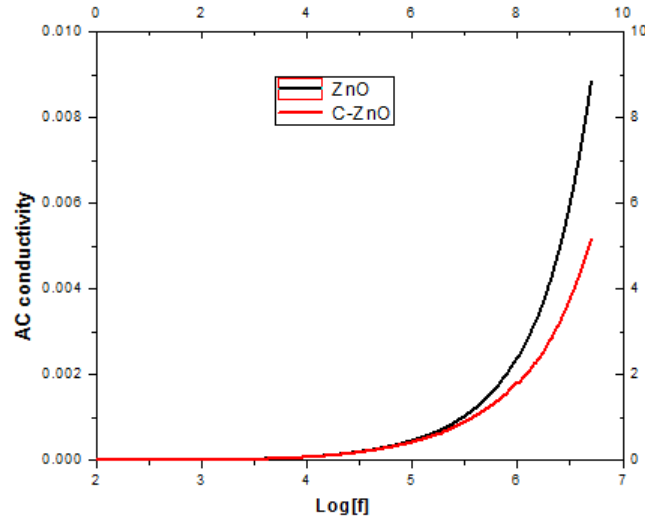
Figure 4.14: AC conductivity for ZnO and C-ZnO as function of frequency

4.7 Spin diffusion length 'l_s' and conductivity

Spin diffusion length can be calculated from dielectric measurement with help of spin transport in material and drift diffusion equation. Spin transport study gives the spin density helping for transport in material, while drift-diffusion equation helps us formulate spin diffusion length. Effective conductivity '$\sigma = \sigma_\uparrow + \sigma_\downarrow$' and spin selectivity is calculated from above equations which as;

$$\sigma = e.(N_{Doping} + n_{accumul}).mobility.2.\cosh(\frac{\mu_{spin}}{kT}) \tag{4.20}$$

$$\beta = \frac{\sigma_\uparrow - \sigma_\downarrow}{\sigma_\uparrow + \sigma_\downarrow} = \tanh(\frac{\mu_{spin}}{kT}) \tag{4.21}$$

σ is the experimental conductivity presented figure 4.14. Finally spin diffusion length l_s is calculated from spin selectivity as;

$$l_s = l_{s,0} \sqrt{1 - \beta^2}$$ (4.22)

Where $l_{s,0}$ is the intrinsic spin diffusion length, calculated from spin coherence time. Spin diffusion length for ZnO and C-ZnO is calculated using the experimental conductivity and dielectric constant of material in table 4.4.

Spin diffusion length for C-ZnO nanowires is greater then ZnO due high dielectric constant. Sudden elevation in spin diffusion length at specific dielectric constant due to rise in electronic polarizability.

Table 4.4: Spin-diffusion length for ZnO and C-ZnO

Temperature (K)	Diameter(nm)		Dielectric constant		AC conductivity (S/m)		l_s (nm)	
	ZnO	CZnO	ZnO	CZnO	ZnO	CZnO	ZnO	CZnO
300	50.29	98.6	154.94	194.80	5.68E-05	0.001028563	18.6687	62.5711
373	50.29	98.6	177.38	317.22	0.00026	0.001150867	3.9984	55.9216
473	50.29	98.6	331.38	406.93	0.000575	0.001291726	2.5288	49.8235

4.8 Overlapping Area between electrons and proposed model for Two-bit quantum gate

Two Qubit gate can be implemented physically by making contact of two nanowires with the help of electrically switching field. During such designing we have to consider the coherence length such that spin for electron remains coherent. This can be done by defining the hamiltonian of our qubit. Two spin interacting by exchange interaction so hamiltonian is defined as;

$$H_{ex} = J(t)\mathbf{S_1}.\mathbf{S_2}$$ (4.23)

where 'J(t)' is the exchange coupling between two electron, which can be turned-on by reducing the inter-wire distance or by lowering between the two electron site. Time evolution of such system

is defined as;

$$U_{ex} = e^{\iota\beta/4} e^{-\iota\beta U_{swap}/2} \tag{4.24}$$

'$U_{swap} = diag(1, \sigma_x, 1)$' and '$\beta = \frac{1}{\hbar} \int_{t_1}^{t_2} J(t)dt$' for $\beta = \pi$ the spin state for two electron is swapped. Its necessary to define the overlapping area in which two electron interact, so electrons moving in 1-dimensional wires situated in xy-plane and are confined in z-direction. Between any external contact it behaves like a free particle, and corresponding hamiltonian is;

$$H_0 = \frac{P^2}{2m^*} + V_0(r) \tag{4.25}$$

$V_0(r)$ is parabolic perpendicular to wires and square potential along z-direction, but we confined the particle in z-direction.

$$H_{orb} = \frac{1}{2m^*}(p_1^2 + p_2^2) + V_c(r_1) + V_c(r_2) + \frac{e^2}{\kappa|r_1 - r_2|} \tag{4.26}$$

Where 'e' is electron charge and κ is the dielectric constant. Along y-direction quartic potential is assumed of the form;

$$V_c(y) = \frac{m^*\omega^2}{8}(y^2 - a^2)^2 \tag{4.27}$$

Thus we can assume the single particle wave function in a single nanowire is;

$$\phi(x, y) = \left(\frac{m^*\omega}{\hbar\pi^2\delta^2}\right)^{\frac{1}{4}} exp(-\frac{x^2}{2\delta^2} - \frac{y^2 m^*\omega}{2\hbar}) \tag{4.28}$$

Inter-wire overlap 'S' is probability of occurrence of two electron in a specified area is;

$$S = \int\int \phi_{+a}^* \phi_{-a} dx dy \tag{4.29}$$

$$= \int\int \sqrt{\frac{m\hbar\omega}{\pi^2\hbar^2\delta^2}} \exp\left(-\frac{x^2}{\delta^2} - \frac{y^2\hbar\omega}{\hbar^2}\right) dx dy \tag{4.30}$$

$$= \frac{\hbar\delta}{4\sqrt{m\hbar\omega}} erf(\frac{x}{\delta}) \left[\sqrt{\frac{m\hbar\omega}{\hbar^2\delta^2}} erf\left(\frac{\sqrt{y}m\hbar\omega}{\hbar}\right)\right] \tag{4.31}$$

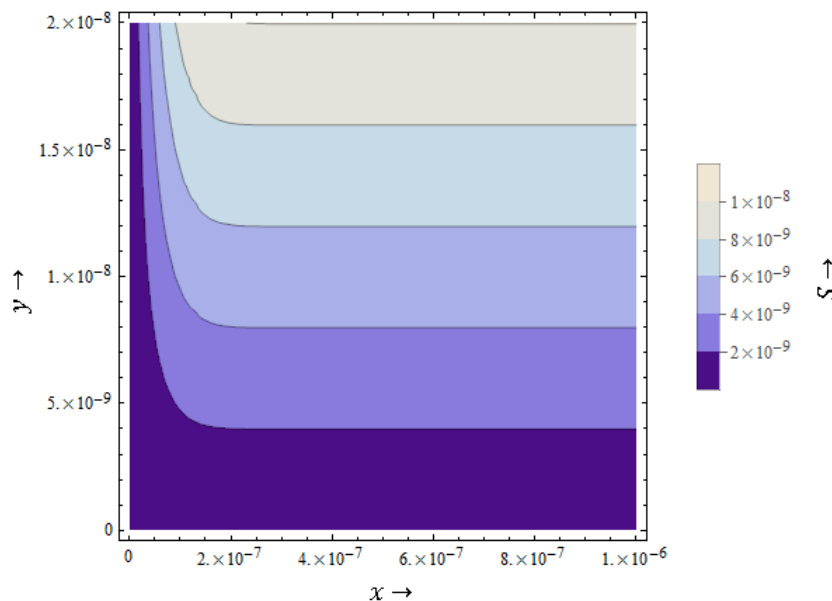Overlapping area is drawn in figure 4.15 for CZnO,

Figure 4.15: Overlapping area of electron in term of inter-wires distance.

As we know from table 4.4 the coherence length for CZnO is feasible for implementing two-qubit gate such as Quantum SWAP gate.

4.8.1 Proposed structure for Quantum Entanglement Device for 2 qubit

When ferromagnetic material is subject to electric field there is momentum dependent spin splitting, state of single spin carrier is defined as; [39]

$$\psi = \alpha| \uparrow> + \beta| \downarrow> \tag{4.32}$$

Two nanowires are used as emitter for two qubit gate which are connected by quantum channel, circuit for such gate is shown in figure 4.16. Properties of this quantum channel such that it preserved long spin diffusion length to keep avoid the state from decoherence. These states are transferred to quantum channel by switching voltage shown in figure 4.17, switching of voltage such that from both two emitters transport different eigenstate ($\uparrow$ or $\downarrow$) to quantum channel, where
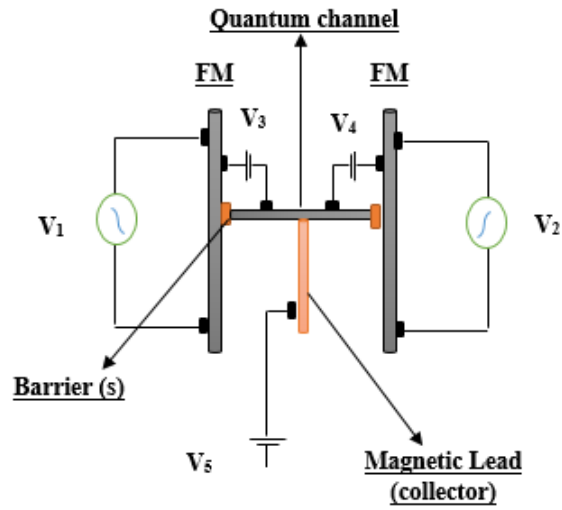
Figure 4.16: Circuit diagram for 2-qubit Gate.

they coupled through exchange interaction. [40, 41] Two possible exchange interaction produces

Figure 4.17: Switching Technique for Voltage V3 and V4.

two different state, where the quantum state of quantum channel is $\psi_{qc} = \alpha| \uparrow > + \beta| \downarrow >$.

$$\psi = | \uparrow > \bigotimes (\alpha| \uparrow > + \beta| \downarrow >) \tag{4.33}$$

$$or$$

$$\psi = | \downarrow > \bigotimes (\alpha| \uparrow > + \beta| \downarrow >) \tag{4.34}$$

Resultant state can be collected through collector (magnetic lead) by potential V_5.

$$\psi = \alpha| \uparrow\downarrow> +\beta| \downarrow\uparrow> \tag{4.35}$$

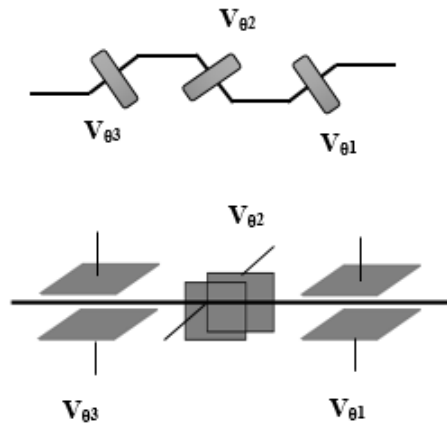Which is a state of two gate bit gate. By controlling the switching potential V_3 and V_4, state on collector can be controlled.

4.9 Summary

Crystallinity of ZnO and CZnO is confirmed by XRD analysis, Band-gap analysis is done by UV-Vis spectroscopy technique, crystal morphology is examined by SEM spectroscopy. While elemental composition and surface bonding is analyzed by using EDX and FTIR spectroscopy. All These result shows that successful nano structure for ZnO and CZnO had been synthesized. And doping of Carbon in ZnO is achieved by tuning the PEG concentration. Dielectric measurement has been performed to measure the dielectric and AC conductivity for ZnO and C-ZnO. Spin coherence length had been calculated by using the effective conductivity approximation. Results for spin diffusion length shows that two-qubit gate can be design by using the exchange interaction.

Chapter 5

Discussion and Outlook

Spin transport can be study by making the analogy between two band model for charge and two channel model for spin, from this analogy spin density can be formulated. Different quantum effects like Rashba spin orbit coupling, spin transfer torque, exchange interaction made spin transport more interesting and useful. Quantum operations are possible in ZnO and C-ZnO due to large spin coherence length and its variation with diameter of nanowires.

By taking the free energy density as function of fractional concentration of bi-phase solution, nucleation theory can be re-produced for 1-D, 2-D and 3-D nano-structures while taking into account the mixing entropy, mixing internal energy and mixing Halmholtz energy as thermodynamic variable. ZnO and C-doped ZnO nanowires are synthesized by using hydrothermal technique, and tuning in diameter is achieved using different percentage of PEG, which is used as surfactant. XRD, SEM and EDX confirms the single phased nanowires with no impurity. Large band gap is observed for ZnO using UV-Vis spectroscopy technique. Dielectric measurement for ZnO and C-ZnO shows that by doping of Carbon in ZnO enhance the ferroelectric properties. Spin coherence length for CZnO is such that two-qubit gate can be physically implemented for quantum computation purposes.

Outlook

Non-Equilibrium Green Function (NEGF) is a powerful technique for studying the spin transport in materials. Graphene (one-layer of carbon atom) has current density six times higher then copper. NEGF along with massless Dirac equation, relativistic quantum mechanics can be used for the Graphene to study the properties like spin-injunction, spin transport etc.

Keeping alive the **Feynman's** saying that is, "it seems that laws of physics present no barrier to reducing the size of computers until the bits are the size of atoms and quantum behavior holds dominant sway". I suggest that there should be race for getting control on nuclear spin because due to spin orbit coupling it contribute to decoherence in electrons. Whereas an isolated nuclear spin has long decoherence time which can be effective for quantum computating.

Topological insulators (TIs) conduct electricity through edges in 2-D and by surfaces in 3-D due to presence of energy state at respective cites. Elastic scattering are in control at edges/surfaces, so time reversal symmetry can be achieved. Through time reversal symmetry one can control the decoherence.

As there are a lot of study available on the physical implementation of qubit using quantum dots, if we control the evolution of quantum dots in 1-dimension then a lot of entanglement can be generated through which enormous computation can be made possible.

Bibliography

[1] J. Gang, Z. Zhang, C. Yanxue, Y. Shishen, L. Yihua, and M. Liangmo, "Current spin polarization and spin injection efficiency in zno-based ferromagnetic semiconductor junctions," *Acta Metallurgica Sinica (English Letters)*, vol. 22, no. 2, pp. 153–160, 2009.

[2] J. Yi, C. Lim, G. Xing, H. Fan, L. Van, S. Huang, K. Yang, X. Huang, X. Qin, B. Wang, *et al.*, "Ferromagnetism in dilute magnetic semiconductors through defect engineering: Li-doped zno," *Physical review letters*, vol. 104, no. 13, p. 137201, 2010.

[3] D. P. DiVincenzo, "Quantum computation," *Science*, vol. 270, no. 5234, p. 255, 1995.

[4] J. Wang, Z. Gu, M. Lu, D. Wu, C. Yuan, S. Zhang, Y. Chen, S. Zhu, and Y. Zhu, "Giant magnetoresistance in transition-metal-doped zno films," *Applied physics letters*, vol. 88, no. 25, p. 2110, 2006.

[5] S. Datta and B. Das, "Electronic analog of the electro-optic modulator," *Applied Physics Letters*, vol. 56, no. 7, pp. 665–667, 1990.

[6] A. Soudi, P. Dhakal, and Y. Gu, "Diameter dependence of the minority carrier diffusion length in individual zno nanowires," *Applied Physics Letters*, vol. 96, no. 25, p. 253115, 2010.

[7] D. P. DiVincenzo *et al.*, "The physical implementation of quantum computation," *arXiv preprint quant-ph/0002077*, 2000.

[8] T. Oosterkamp, S. Godijn, M. Uilenreef, Y. V. Nazarov, N. Van der Vaart, and L. P. Kouwenhoven, "Changes in the magnetization of a double quantum dot," *Physical review letters*, vol. 80, no. 22, p. 4951, 1998.

[9] B. E. Kane, "A silicon-based nuclear spin quantum computer," *nature*, vol. 393, no. 6681, pp. 133–137, 1998.

[10] R. Vrijen, E. Yablonovitch, K. Wang, H. W. Jiang, A. Balandin, V. Roychowdhury, T. Mor, and D. DiVincenzo, "Electron-spin-resonance transistors for quantum computing in silicon-germanium heterostructures," *Physical Review A*, vol. 62, no. 1, p. 012306, 2000.

[11] N. H. Bonadeo, J. Erland, D. Gammon, D. Park, D. Katzer, and D. Steel, "Coherent optical control of the quantum state of a single quantum dot," *Science*, vol. 282, no. 5393, pp. 1473–1476, 1998.

[12] M. Žnidarič, "Spin transport in a one-dimensional anisotropic heisenberg model," *Physical review letters*, vol. 106, no. 22, p. 220601, 2011.

[13] M. E. Flatté and I. Tifrea, *Manipulating quantum coherence in solid state systems*, vol. 244. Springer Science & Business Media, 2007.

[14] D. Maslov, A. Chubukov, and V. Yudson, "Optical conductivity of a two-dimensional metal at the onset of spin-density-wave order," in *APS Meeting Abstracts*, vol. 1, p. 46004, 2014.

[15] I. Chuang, R. Laflamme, P. Shor, and W. Zurek, "Quantum computers, factoring, and decoherence," *arXiv preprint quant-ph/9503007*, 1995.

[16] T. Takagahara, *Quantum Coherence Correlation and Decoherence in Semiconductor Nanostructures*. Academic Press, 2003.

[17] D. D. Awschalom, D. Loss, and N. Samarth, *Semiconductor spintronics and quantum computation*. Springer Science & Business Media, 2013.

[18] M. Isasa, E. Villamor, L. E. Hueso, M. Gradhand, and F. Casanova, "Temperature dependence of spin diffusion length and spin hall angle in au and pt," *Physical Review B*, vol. 91, no. 2, p. 024402, 2015.

[19] M. Caglar, S. Ilican, Y. Caglar, and F. Yakuphanoglu, "Electrical conductivity and optical properties of zno nanostructured thin film," *Applied Surface Science*, vol. 255, no. 8, pp. 4491–4496, 2009.

[20] Y. Yang, W. Guo, X. Wang, Z. Wang, J. Qi, and Y. Zhang, "Size dependence of dielectric constant in a single pencil-like zno nanowire," *Nano letters*, vol. 12, no. 4, pp. 1919–1922, 2012.

[21] T. Dietl, H. Ohno, and F. Matsukura, "Hole-mediated ferromagnetism in tetrahedrally coordinated semiconductors," *Physical Review B*, vol. 63, no. 19, p. 195205, 2001.

[22] H. Pan, J. Yi, L. Shen, R. Wu, J. Yang, J. Lin, Y. Feng, J. Ding, L. Van, and J. Yin, "Room-temperature ferromagnetism in carbon-doped zno," *Physical review letters*, vol. 99, no. 12, p. 127201, 2007.

[23] M. Aziz, A. Mostafa, A. Youssef, and S. Youssif, "Electrical conductivity and dielectric properties of bulk glass v 2 o 5 (zno, pbo) sro feo," *Physics Research International*, vol. 2011, 2011.

[24] M. Althammer, E.-M. Karrer-Müller, S. T. Goennenwein, M. Opel, and R. Gross, "Spin transport and spin dephasing in zinc oxide," *Applied Physics Letters*, vol. 101, no. 8, p. 082404, 2012.

[25] J. Jaffe and A. Hess, "Hartree-fock study of phase changes in zno at high pressure," *Physical Review B*, vol. 48, no. 11, p. 7903, 1993.

[26] P. Yang, H. Yan, S. Mao, R. Russo, J. Johnson, R. Saykally, N. Morris, J. Pham, R. He, H.-J. Choi, *et al.*, "Controlled growth of zno nanowires and their optical properties," *Advanced Functional Materials*, vol. 12, no. 5, p. 323, 2002.

[27] A. Moezzi, A. M. McDonagh, and M. B. Cortie, "Zinc oxide particles: Synthesis, properties and applications," *Chemical Engineering Journal*, vol. 185, pp. 1–22, 2012.

[28] S.-H. Wei and A. Zunger, "Role of metal d states in ii-vi semiconductors," *Physical Review B*, vol. 37, no. 15, p. 8958, 1988.

[29] Z. Fan, D. Wang, P.-C. Chang, W.-Y. Tseng, and J. G. Lu, "Zno nanowire field-effect transistor and oxygen sensing property," *Applied Physics Letters*, vol. 85, no. 24, pp. 5923–5925, 2004.

[30] J. W. Park, D. H. Kim, S.-H. Choi, M. Lee, and D. Lim, "The role of carbon doping in zno," 2010.

[31] N. Ashkenov, B. Mbenkum, C. Bundesmann, V. Riede, M. Lorenz, D. Spemann, E. Kaidashev, A. Kasic, M. Schubert, M. Grundmann, *et al.*, "Infrared dielectric functions and phonon modes of high-quality zno films," *Journal of applied Physics*, vol. 93, no. 1, pp. 126–133, 2003.

[32] D. Turnbull and R. Cech, "Microscopic observation of the solidification of small metal droplets," *Journal of Applied Physics*, vol. 21, no. 8, pp. 804–810, 1950.

[33] B. Vinet, L. Magnusson, H. Fredriksson, and P. J. Desré, "Correlations between surface and interface energies with respect to crystal nucleation," *Journal of colloid and interface science*, vol. 255, no. 2, pp. 363–374, 2002.

[34] E. Matijević and D. Goia, "Formation mechanisms of uniform colloid particles," *Croatica Chemica Acta*, vol. 80, no. 3-4, pp. 485–491, 2007.

[35] R. Koch, D. Winau, A. Führmann, and K. Rieder, "Growth-mode-specific intrinsic stress of thin silver films," *Physical Review B*, vol. 44, no. 7, p. 3369, 1991.

[36] D. Turnbull and J. C. Fisher, "Rate of nucleation in condensed systems," *The Journal of chemical physics*, vol. 17, no. 1, pp. 71–73, 1949.

[37] R. Lieth, *Preparation and crystal growth of materials with layered structures*, vol. 1. Springer Science & Business Media, 1977.

[38] S. F. Burlatsky, V. V. Atrazhev, D. V. Dmitriev, V. I. Sultanov, E. N. Timokhina, E. A. Ugolkova, S. Tulyani, and A. Vincitore, "Surface tension model for surfactant solutions at the critical micelle concentration," *Journal of colloid and interface science*, vol. 393, pp. 151–160, 2013.

[39] A. Barenco, D. Deutsch, A. Ekert, and R. Jozsa, "Conditional quantum dynamics and logic gates," *Physical Review Letters*, vol. 74, no. 20, p. 4083, 1995.

[40] S. Mohammad Nejad and M. Mehmandoost, "Realization of quantum hadamard gate by applying optimal control fields to a spin qubit," in *Mechanical and Electronics Engineering (ICMEE), 2010 2nd International Conference on*, vol. 2, pp. V2–292, IEEE, 2010.

[41] A. Popescu and R. Ionicioiu, "All-electrical quantum computation with mobile spin qubits," *Physical Review B*, vol. 69, no. 24, p. 245422, 2004.